**DECEMBER 2002**

Progress Report

1.1 2001 – 16.12 2002

Technion Project No 160 – 911

Submitted to Ministry of Sciences and Culture of Niedersachsen

# The Number and Speed of Stall Cells During Rotating Stall in a Multi-Stage Compressor

**Joseph Pismenny** and **Yeshayahou Levy**

*The Turbo and Jet Engine Laboratory*
*Faculty of Aerospace Eng., Technion , Israel Institute of Technology*

*Haifa 32000, Israel*

**TAE No 906**

**JTL 002-12-2002**

---

## Table of contents

## ABSTRACT

*The number of stall cells and their rotation speed are distinctive features of the rotating stall phenomenon and play an important role in the predictions and analysis of the pressure fields during the rotating stall. Different aspects of these characteristics are analyzed. It is shown that whereas the numbers of stall cells in different transverse cross-sections of a multistage compressor may vary, the pressure fields' rotational speeds and accordingly the rotation speeds of all stall cells seem to be the same.*


## NOMENCLATURE

$k$ - number of stall zones in transverse cross-section
$n$ – number of pressure oscillation periods during one cell rotation period
$t$ - time
$T$ - period
$\omega$ - frequency
$\varphi$ - change of pressure oscillation phase in transverse cross-section
$\theta$ - compressor stator angle relative to its axis
$\tau$ - duration

**Subscripts**
*OSC*- pressure oscillation
*rot* – rotor rotation
*CR* – cells rotation

## 1. INTRODUCTION

The stall cells (stall zones) and the cell rotation speed are distinctive features of the rotating stall phenomenon. The interpretation of the experimental data and calculation results play an important role in the analysis of the pressure and velocity fields during rotating stall. The number of stall cells mentioned in published experimental and theoretical studies of rotating stall may be one, two, three and even more (see for example Ciannissis et al, 1992, Day, I.J., 1992, Day and Freeman, 1994, Ehrich et al., 2001, Inoue et al., 2000, Inoue et al., 2002, Levy et al., 2002, Mathioudakis and Breugelmans, 1985, Poensgen and Gallus, 1996, Storace et al, 2001).

The number of stall cells and their rotational speeds is not the main subject in most papers. However, relevant parameters may be obtained from these papers. For example Inoue et al., 2002, examine the short and long length-scale disturbances leading to rotating stall in an axial compressor stage. We can consider the short length-scale disturbance as the vortices from the rotor blades and the long length-scale disturbances as the disturbances directly related to the stall process. Therefore, the frequency of the short length-scale disturbances may be that of the rotor blade frequency. Consequently, the frequency of the long length-scale disturbances is the frequency of rotating stall processes and is in the order of rotor rotational frequency.

The number of pressure sensors in experiments with compressors is usually limited. However, recent advances in sensor technology allow recordings of massive amounts of pressure signal data. The problem with such data analysis lies in possible misinterpretations. Hence there is a need to improve the techniques for interpretation of the pressure and velocity fields within the compressor during rotating stall that would allow accurate definition of the number of stall cells and their rotation speeds. However, it is our understanding that in order to achieve accurate and meaningful results one needs simultaneous analysis by visual interpretation of the pressure oscillations in time and space together with other characteristics (for example, the frequency spectra).

## 2. IDEALIZED MODELS OF STALL CELLS

### Pressure change in time

First there is a need to define a stall cell (stall zone), by pressure field analysis. All pressures have periodical components during steady-state rotating stall processes. We designate the regions of significant pressure reductions in the pressure signal as stall cells. We relate to the lower part of pressure oscillation as stall because stall is always accompanied by pressure reduction. Thus, we can name the regions in the pressure fields of lower values as rotating cells. Typically, the first harmonic amplitude in the pressure spectra is larger than all other harmonic amplitudes.

The pressure characteristics become complicated due to higher and lower harmonics in the pressure signals which may also include contributions from rotor blade rotation. In order to simplify the analysis, we first consider several examples of idealized pressure behavior in a transverse cross-section of a compressor during rotating stall. Figures 1-3 show three typical examples of pressure behavior:

a) Sinusoidal curve of pressure change (Fig. 1). This form may also be found in cases of filtered pressure signals.

b) Quasi-steady pressure with discrete pressure decrease (pulse, Fig. 2). The shape of the pulse may be of different form (linear, exponential) - this is incidental.

c) Quasi-steady pressure variations with sets of a few pressure decreasing pulses or continuous pressure pulses (Fig. 3). Similar cases are described, for example in Inoue et al., 2002.

We should distinguish between cases of a certain number of continuous pulses within the period of pressure field rotation (repetition of the pressure field) from a similar number of pulses in a period, but in separated groups of pulses. (See for example the case of three groups with four pulses in the pressure field period (Fig. 3a) and the case of twelve continuous pulses in the period (Fig. 3b).)

It is clear that only a whole number of stall cells may exist simultaneously in any transverse cross-section of the compressor. Hence, the instantaneous pressure distribution in the circumference of the compressor section begins and ends at the same point, and must include the information about all existing cells. Theoretically the value of these whole numbers is not limited. However, it is limited in practice during rotating stall. The number of stall cells should be less than the rotor blade number, because oscillations with blade frequencies are induced from blade whirls and therefore relate to other phenomenon (see Inoue et al., 2001, Inoue et al., 2002, Storace et al., 2001).

**Transfer from pressure change in time to pressure change in circumference of compressor**

We introduce the following interpretation: the characteristic of pressure variations in circumference of a specific transverse cross-section at a specific time appears to be similar to the characteristic of pressure variation with time at a certain location on the compressor circumference. The number of low-pressure regions within the pressure field (over the compressor circumference), defines the number of stall sells. Hence the simultaneous information about the pressure variation in time at several points on the compressor circumference includes also the information about the pressure fluctuation in the compressor circumferential direction. Hence, a minimum of two sensors on the compressor circumference is needed during experiments in order to determine the relation between the phases of pressure signals and the sensor locations. For such analysis, the rotor and stall cell speeds are of no practical importance.

For definition of pressure variations at the circumference of a compressor, a large number of sensors must be installed in a single transverse cross-section of the compressor stator. The accuracy of this characteristic will increase with increased number of sensors. It is a fact that the pressure fluctuations (with time) at different points of the compressor circumference, during steady state rotating stall processes are similar, however with different time shift. The values of these time shifts (or phase shifts) depend on the geometrical angles between the sensor locations on the compressor casing in the transverse cross-section. The link between the phases of pressure oscillation and the geometrical angles of the sensor locations depends also on the number of stall cells. Figures 4 and 5a show in polar coordinates a few examples of idealized pressure signal corresponding to cases of one and two stall cells with

sinusoidal curve of pressure change (Figs. 4a and 4b) and cases of one and two pulse signals of pressure (Fig. 4c – for one stall cell, Fig. 4d – for two symmetric stall cells, and Fig. 5a – for an asymmetry case of two cells). As can be seen from these figures, the links between the phases of pressure oscillation and the geometrical angles of the sensor locations are determined by the number of cells. Accordingly the numbers of cells may be defined from the experimentally obtained characteristic "phases of pressure oscillation with respect to the sensor location". Examples of these characteristics will be given later in the paper.

The other method for the determination of the number of stall cells in a transverse cross-section is to be found in graphs of the pressure variations in this cross-section during rotating stall as shown in Figs. 1 and 2 (with intervals between the lines of pressure variation signals proportional to angles between the sensors and repetition of one signal twice). One needs to graph a line via similar points in signals of all sensors and determine the period of field or cells rotation, $T_{CR}$ , as shown in these figures. The number of periods of pressure oscillation, $T_{OSC}$, during period of cells rotation, $T_{CR}$ ,

$$n = \frac{T_{CR}}{T_{OSC}}.$$

This may be used for determination of the number of stall cells in a transverse cross-section, *k.* In most cases we find

$$k = n.$$

However in specific cases of more complicated forms of signals (for example see Fig. 5):

$$k = 2n,\ k = 3n,\ \ldots$$

**The speed of stall cell rotation**

The speed of stall cell rotation, $\omega_{CR}$ , (for each of the cells and at different rotor speed) is defined by two parameters:

1) the angle of pressure field rotation, $\Delta\theta$,
2) the duration of this angle of pressure field rotation $\Delta\tau$.

Consequently:

$$\omega_{CR} = \frac{\Delta\theta}{\Delta\tau}.$$

The pressure field as demonstrated by any of the sensors located in a specific stator cross-section repeats itself periodically. Hence a period of the pressure field rotation may be determined. It should be remembered that within one cycle of the pressure field rotation there may be several cells (different in their intensity and size; see for example Fig. 5). It is the authors' opinion that in practice these cells can be similar or different. However, the formulae for determination of the cells rotational speed, $\omega_{CR}$ , for all cases must be the same. It should also be remembered that there is no direct link between the speed of rotor rotation and that of the pressure field rotation. Consequently, in an exact analysis, the different cells should be considered individually and each one of them would rotate at the same speed as the whole pressure field. However, sometimes the different cells may seem similar and evenly distributed in the circumference. Even in such a case the period for the cell cycle

should be considered as that of the global pressure field rotation, as determined from the phase correlation between sensors located at different circumferential positions.

The pressure field rotational period ($T_{CR}$)

- may be equal to the period of pressure oscillation in time $T_{OSC}$ (case of single cell rotation; see Figs. 1, 4a, 4c);
- may be greater than the period of pressure oscillation $T_{OSC}$ in whole number $k$ (for example the case of two similar cells rotating simultaneously ( $k = 2$) (see Figs. 2, 4b, 4d);
- may be equal to the sum of time duration of the different pressure oscillating cells (in case of several different asymmetrical cells see Fig. 5b);
- cannot be less than the period of pressure oscillation $T_{OSC}$. This is impossible because the phase of pressure field oscillation must repeat itself in time $t = 0$ and in time $t = T_{CR}$ .

In case of idealized pressure fields (as seen in Fig. 4), the minimal angle at which the characteristic pressure versus angular position of the sensor at the compressor stator is repeated may be equal $\frac{2\pi}{k}$, where $k$ is the number of stall cells. However, in reality, due to differences even between "similar" cells the period is exactly $2\pi$. This may be as a result of the fact that the parameters of different cells may be not identical. (See the example in the following section of the paper.)

## 3. ANALYSIS OF EXPERIMENTAL DATA ABOUT STALL CELLS AND THEIR ROTATION SPEEDS

There are different methods to interpret experimental data. However, it is our opinion that visual analysis of pressure oscillation signals in time and space in conjunction with additional methods such as frequency spectral analysis may give the correct results. The present study refers to interpretation of experimental data obtained during rotating stall in a four-stage axial compressor of the University of Hanover. More detailed characteristics of this compressor and these experiments may be found in Levy et al., 2002, Pismenny and Levy, 2001. A longitudinal cross-section of the compressor with numbering of sensors in transverse cross-sections and a circumferential cross-section of the compressor with angular numbering of sensors are given in Fig. 6.

### Rotating stall with different numbers of cells in different transverse cross-sections

*Single cell*. Fig. 7 shows pressure changes over the circumference of the compressor during an established process of rotating stall in transverse cross-sections #1 (four sensors: F1, G1, A1, B1 with repetition of sensor F1). The pressure change of sensor F1 is shown twice to show the pressure behavior of the whole circumference of the cross-sections. The rotating stall was perceived at a rotor speed of about 14400 rpm (i.e. 240 Hz or 80% of the design rotor speed 18000 rpm). It is seen from the figure that:

a) The pressure field rotational period is equal to the period of pressure oscillation in this cross-section (0.0097 s, one cell).

b) We may consider also this duration as equal to the period of the cell rotation, $T_{CR}$. This means that the frequency of cell rotation in this cross-section, $\omega_{CR}$, equals about 103 Hz.

This process would be considered as a typical rotating stall process with one rotating cell.

*Multiple Cells*. Considering the pressure changes over the compressor length (sensors F1, F2, F1, F2, F3, F4, F5, F6, F7, F8, F9; see Fig. 8) and the frequency spectra of these pressure signals (see Fig. 9) we see that:

a) The first harmonic of pressure oscillations has the maximal values of amplitudes for sensors in transverse cross-sections #1, #2, #3, #6 and #9 (sensors F1, F2, F3, F6, and F9).

b) The second harmonic of pressure oscillations has the maximal values of amplitudes for sensors in transverse cross-sections #4, #5 and #7 (sensors F4, F5, F7). The amplitudes of the first harmonic in these cross-sections are substantially smaller than the amplitudes of the second harmonic.

c) In cross-section #8 (sensor F8), both amplitudes of the first and second harmonics of pressure oscillations are large.

From the signals in Fig. 8 and in accordance with the cell definition in part 2 of the paper it seems that in cross-sections #1, #2, #3, #6 and #9 there are one cell in each cross-section and in cross-sections #4, #5 and #7 there are two cells. These characteristics can also be interpreted from the frequency spectra of the time signals (Fig. 9). Whenever the first harmonic is largest in amplitude, there is only one cell. When the second harmonic is dominant, two cells rotate simultaneously within a compressor cross-section. Consequently, it seems that in order to obtain the correct interpretation of the pressure signal and the rotating stall behavior, there is a need to consider a large number of stages (and their frequency characteristics) in several cross-sections and during common time.

A different and novel way to present the data and to visually display the cell's dynamics is presented in Fig. 10. Figure 8 shows the time variation of pressure signals from sensors in all transverse cross-sections. Let us consider for example the pressure signals only in three specific cross-sections: cross-section #1 (signal F1 with one cell during period of pressure oscillation), in cross-section #7 (signal F7 with two cells during period of pressure oscillation), and in cross-section #9 (signal F9 with one cell during period of pressure oscillation). If we multiply the time by the angular frequency of the pressure field rotation, $\omega_{CR}$ (about 103 Hz, interpreted previously), we may display the pressure signals from the different sensors and at a certain/the same time as a function of the angular position. Hence the polar distributions of these pressure signals may be regarded as the pressure fields that exist at different instance of time (see Figs 10a, 10b and 10c). The parts of the polar curves close to the center of the diagram represent the stall cells region. As may be seen in Figs. 10a and 10c only one stall cell exists in cross-sections #1 and #9 (according to the signals of sensors F1 and F9) and two stall cells exist in cross-sections #7 (according to the signal of sensors F7).

If we filter the signals displayed in Figs. 10a, 10b and 10c by a band-pass filter for the first harmonic we could visualize the existence of one rotating cell. This result is shown in Figs. 10d, 10e and 10f. For analysis of these figures, one must draw

attention to the scales of the diagrams. (For example the maximum scale of the diagram in Fig. 10d (0.5) is 10 times larger than the minimum scale of the diagram in Fig. 10e (0.05).) Accordingly, we also see from this characteristic that one stall cell exists in cross-sections #1 and #9 and practically does not exist in cross-section #7.

However, if we apply a filter for the second harmonic (about 206 Hz), we clearly see the existence of two cells rotating simultaneously (see Figs. 10g, 10h and 10i). We also see from this characteristic that two stall cells exist in cross-sections #7 and practically do not exist in cross-sections #1.

We may assume that all cells in all cross-sections rotate simultaneously with rotation speeds equal to the frequency of the first harmonic of pressure oscillations. Thus, we see that in all transverse cross-sections, the speed (or frequency) of stall cell rotation is equal to the frequency of the first harmonic of pressure oscillations - about 103 Hz. In addition, it seems that wherever there are several cells, they all rotate at the same speed (for example in cross-sections #7). Figure 11 shows correlations between the phase of pressure oscillation, $\varphi$, and the positions of sensors G1, A1, B1 relative to sensor F1 (angle $\theta$) in transverse cross-section #1, for the first harmonic. This characteristic is linear.

Hence, we see that based on Figs. 9-11 we may assume the following:

- There is one stall zone in cross-sections #1, #2, #3, #6 and #9.
- There are two stall zones in cross-sections #4, #5 and #7.
- The rotation speeds of the pressure fields in all cross-sections are equal.

**Rotating stall with three zones**

Figures 12 and 13 show fragments of pressure variations in a compressor during an established process of rotating stall (in test 18, 17100 rpm or 95% of design rotor speed -18000 rpm). Figure 12 shows the pressure changes in the compressor during an established process of rotating stall in longitudinal cross-section (four sensors: F1, F2, F4, F6). Figure 13 shows the pressure changes in the compressor in transverse cross-section (four sensors: F1, G1, A1, D1). The first harmonics of pressure signals in transverse cross-section (Fig. 14) are received after filtering these four signals (F1, G1, A1 and D1).

Figure 15 shows the change of phase characteristic of the first harmonic of pressure in the transverse cross-section versus positions of sensors (G1, A1, and D1 relative to sensor F1). All characteristics shown in Figs. 16-19 may be graphed only after that of Fig. 15 and the definition from this figure of the number of stall cells

$$k = n = \frac{1080}{360} = 3.$$

Figures 16 and 17 show the equivalent pressure variations in polar coordinates. Figures 18 and 19 respectively show in polar coordinates, variations of the first harmonics of these pressures. The effect of rotor blades of the first rotor stage (fluctuating pressure values) are clearly visible in Figs. 13 and 14, and especially in Figs. 16 and 17, but they are not stall cells. We can see in Figs. 16 and 18 that the pressure variations, and correspondingly the first harmonics of the pressure variations, in four points (F1, G1, A1, D1) of one transverse cross-section (in this case - first), are

not absolutely identical, but identical enough in order to view them as rotations of the same characteristics.

As may be seen, the frequency of pressure oscillation is about 1570 Hz. At the same time the speed (or frequency) of stall cell rotation, $\omega_{CR}$, is three time less - 523 Hz. This is because of the fact that the period of the stall cells rotation is equal to three periods of pressure oscillation.

**Blade rotor frequencies in pressure oscillation spectra.**

The pressure oscillations with frequencies of rotor blades complicates the total picture of oscillation during rotating stall and needs to be taken into consideration in rotating stall studies (Figs. 13, 14, 16 and 17). Extending the span of the frequency spectra from the pressure signals enables one to include the effect of blade rotor frequencies. Figure 20 demonstrates the frequency characteristics of pressure in a compressor during rotating stall at 60% of designed rotor speed. This figure shows the frequency characteristics of pressure along the compressor (sensors F1 - F2 - F4 - F6 - F8), in the compressor stator circumference (sensors E2 - F2; F1- G1- A1- D1) and over rotor blades in the first rotor stage (sensor R-1) during rotating stall.

As may be seen from the frequency spectra, the frequencies where the oscillation amplitudes obtain large values, correspond to half of the rotor harmonic and to $23^{rd}$, $27^{th}$, $29^{th}$ rotor harmonics (i.e. they correspond to the rotor blade frequencies and are induced from blade whirl). It is a fact that the numbers of rotor blades in the experimental compressor are 23, 27, 29, 31 in the 1, 2, 3, 4 successive blade rows (see Levy et al., 2002). In this experiment, the frequency of maximal oscillation amplitudes during rotating stall equals half the rotor harmonic and accordingly is much less than the rotor blade harmonics.

**Some features of rotating stall with different numbers of cells in different transverse cross-sections**

In previous sections conclusions about cell numbers in different transverse cross-sections were reached on the basis of analysis of only one signal in each of these cross-sections. Below is given an example of measurements for confirming this conclusion. Fig. 21 shows the pressure variations during rotating stall received at rotor speed of about 12600 rpm (i.e. 210 Hz or 70% of the design rotor speed 18000 rpm).

Fig. 22 shows pressure variations over the circumference of the compressor during an established process of rotating stall in transverse cross-sections #4 (four sensors: F4, G4, A4, B4 with repetition of sensor F4) and #5 (four sensors: F5, G5, A5, B5 with repetition of sensor F5). As in Fig. 7 for sensor F1, the parameters of sensors F4 and F5 are shown twice to demonstrate the pressure behavior of the whole circumference of the cross-sections.

It is seen from the figures that:

a) The pressure field rotational period equals the period of pressure oscillation, $T_{OSC}$ (about 0.011s).

b) We may consider these durations as equal to the periods of the cell rotations, $T_{CR}$ . This means that the frequency of cell rotation is the same in the two different cross-sections and equals about 90 Hz.

c) The two stall cells which are situated in the circumference of the cross-sections #5 and #7 are not symmetrical. The durations between two stall cells are not equal to a half period of pressure oscillation:

$$T_{OSC} = \tau_1 + \tau_2, \quad \text{where} \quad \tau_1 \neq \tau_2 .$$

For comparison, consider now (Fig. 23) the frequency spectra of the pressure signals measured by these sensors and presented in Fig. 21. We see that:

a) The maximal amplitudes of pressure oscillations for sensors in transverse cross-section #4 (four sensors: F4, G4, A4, B4) have frequencies of about 90 Hz (the first harmonic of pressure oscillations) and about 180 Hz (the second harmonic).

b) The maximal amplitudes of pressure oscillations for sensors in transverse cross-sections #5 and #7 (four sensors: F5, G5, A5, B5 and F7) have a frequency of about 180 Hz (the second harmonic). The amplitudes of frequencies of about 90 Hz (the first harmonic) are substantially smaller than the amplitudes of the second harmonic.

It seems that there is a possibility for incorrect interpretation (that the frequency of cell rotation becomes formed by the second harmonic). Thus there is a need to consider the frequency characteristics in several cross-sections and in common time.

A different way to display the cell dynamics visually is presented in Figs 24 and 25. Fig. 24a shows time variation of pressure signals from 4 sensors in transverse cross-section #4 (A4, B4, F4 and G4). A section in time ($T_{CR}$ ) from each of these signals is converted to be displayed in polar coordinates in Fig. 24b. Hence the polar distributions of the pressure signals may be regarded as ones obtained at different instances of time where the time delay is related to the relative angular positions of the different sensors. Similarly Fig. 25 shows pressure variations from 4 sensors in transverse cross-section #5 (A5, B5, F5, G5), in time coordinates (Fig. 25a) and also in polar angular coordinates (Fig. 25b).

Fig. 26 shows in polar coordinates the filtered pressure signals variations in transverse cross-section #4 for the first (Fig. 26a) and second (Fig. 26b) harmonics. Similarly Fig. 27 shows in polar coordinates the filtered signals variations from 4 sensors in transverse cross-section #5 (A5, B5, F5, G5), for the first (Fig. 27a) and second (Fig. 27b) harmonics. Thus we see that in all transverse cross-sections, the speed (or frequency) of stall cell rotation is equal to the frequency of the first harmonic of pressure oscillations – about 90 Hz. Fig. 28 shows correlations between the sensor positions relative to the sensors F4 and F5 and changes of their pressure oscillations phases for first (Figs 28a, 28c) and second (Figs 28b, 28d) harmonics.

We may assume based on Figs 24-28 the following: there are simultaneously one stall cell (with frequency of about 90 Hz - the first harmonic) and two stall cells (with frequency of about 180 Hz - the second harmonic) in all examined cross-sections. However the amplitude of the stall cell with frequency of first harmonic in cross-section #5 is substantially smaller than the amplitude of the stall cell with frequency of the second harmonic. We see that the conclusions about the numbers of stall cells are mostly subjective. Therefore it is necessary to mention what one must

take into consideration. First of all, it is necessary to undertake common analysis of rotating stall characteristics (such as the frequency spectra) viewing process in time and space.

The questions that need answers in further investigations are:

a) What may be the reason of different numbers for stall cells in different transverse cross-sections?

b) Why are two stall cells situated in the circumference of cross-sections #5 and #7 not symmetrical and, consequently, the durations between these stall cells not equal to half a period of pressure oscillation?

## CONCLUSIONS

1. The frequency of pressure oscillation and the frequency of cell rotation are different parameters and may have identical or different values.
2. It seems that visual analysis of rotating stall oscillations in time and space in conjunction with other methods (for example the method of frequency spectra) is critical to obtain the correct determination of the number of stall cells and their rotation speeds.
3. In complex cases, the number of stall cells in any transverse cross-section may be defined after graphing the characteristics "phase of pressure oscillation versus sensor positions" and their joint analysis with the pressure signal variations in time and space.
4. The numbers of stall cells in different transverse cross-sections of a multistage compressor may not be identical, however their pressure fields rotate at the same speed and, accordingly, the rotational speeds of the stall cells can be the same.
5. In case of $k$ identical stall cells, the rotational speeds of the stall cells are $k$ times less than the frequency of pressure oscillation.
6. The total picture of pressure oscillation during rotating stall is complicated by the high frequency of the rotor blades. However, this needs to be taken into consideration in rotating stall studies.
7. The questions that need answers in further investigations are:
   a) What may be the reason of different numbers for stall cells in different transverse cross-sections?
   b) Why are two stall cells situated in the circumference of cross-sections not symmetrical and, consequently, the durations between these stall cells not equal to half a period of pressure oscillation?

## ACKNOWLEDGMENT

We would like to thank the Ministry of Sciences and Culture of Niedersachsen, Germany, and the Israeli Ministry of Immigrant Absorption for supporting this research. In addition, we would also like to thank Prof. W. Riess, Prof. J. Seume and Mr. A. Reissner (University of Hanover, Germany) for providing experimental data for analysis and Mr. V. Ognev for preparation of the experimental data for analysis.

## REFERENCES


1. Ciannissis, G.L., McKenzie, A.B., and Elder, R.L., 1992, "Experimental Investigation of Rotating Stall in a Mismatched Three-Stage Axial Flow Compressor", in book "Axial Flow Compressor", Lecture Series 1992-02, von Karman Institute for Fluid Dynamics, pp. 1-18.
2. Day, I.J., 1992, "Stall and Surge in Axial Flow Compressor", in book "Axial Flow Compressor", Lecture Series 1992-02, von Karman Institute for Fluid Dynamics, pp. 1-55.
3. Day, I.J., and Freeman, C., 1994, "The Unstable Behavior of Low and High-Speed Compressors". J. of Turbomachinery, Vol. 116, pp. 194-201.
4. Ehrich, F.F., Spakovszky, Z.S., Martinez-Sanchez, M., Song, Wisler, D.C., Storace, A.F., Shin, H.-W., and Beacher, B.F., S.J., 2001, "Unsteady Flow and Whirl-Induced Forces in Axial-Flow Compressors: Part 2 - Analysis". J. of Turbomachinery, Vol. 123, pp. 446-452.
5. Inoue, M., Kuroumaru, M., Tanino, T., and Furukawa, M., 2000, "Propagation of Multiple Short-Length-Scale Stall Cells in an Axial Compressor Rotor". J. of Turbomachinery, Vol. 122, pp. 45-54.
6. Inoue, M., Kuroumaru, M., Yoshida, S., and Furukawa, M., 2002, "Short and Long Length-Scale Disturbances Leading to Rotating Stall in an Axial Compressor Stage with Different Stator/Rotor Gaps". J. of Turbomachinery, Vol. 124, pp. 376-384.
7. Levy, Y., Pismenny, J., Reissner, A., Riess, W., 2002, "Experimental Study of Rotating Stalls in a Four-Stage Axial Compressor", GT-2002-30362. Proceedings of ASME TURBO EXPO 2002, 47th International Gas Turbine and Aeroengine Congress and Exhibition, 3-6 June 2002, Amsterdam, the Netherlands, 10p.
8. Mathioudakis, K., and Breugelmans, F.A.E., 1985, "Development of Small Rotating Stall in a Single Stage Axial Compressor", ASME paper 85-GT-227.
9. Pismenny, J., and Levy, Y., 2001, "Oscillation in f Multistage Axial Compressor during Rotating Stall". Progress Report No 868. Technion, Haifa, pp. 103.
10. Poensgen, C.A., and Gallus, H.E., 1996, "Rotating Stall in a Single-Stage Axial Flow Compressor". J. of Turbomachinery, Vol. 118, pp. 189-196.
11. Storace, A.F., Wisler, D.C., Shin, H.-W., Beacher, B.F., Ehrich, F.F., Spakovszky, Z.S., Martinez-Sanchez, M., and Song, S.J., 2001, "Unsteady Flow and Whirl-Induced Forces in Axial-Flow Compressors: Part I - Experiment". J. of Turbomachinery, Vol. 123, pp. 433-445.

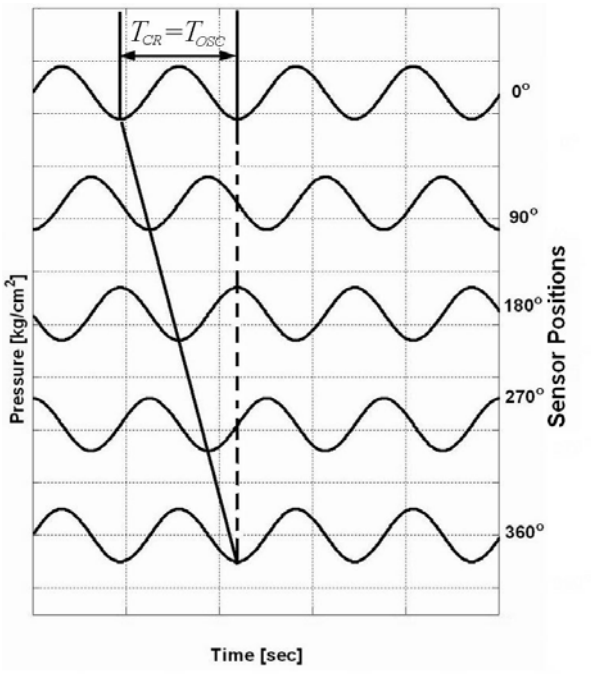


Fig. 1. Idealized characteristic of pressure variations versus time. 4 sensors. Sinusoidal curves of pressure oscillations. Single stall cell ($T_{CR} = T_{OSC}$).

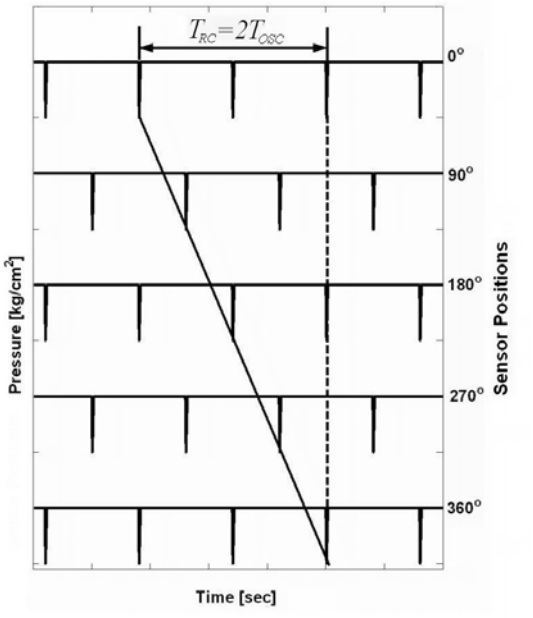


Fig. 2. Idealized characteristic of pressure variations versus time. 4 sensors. Pressure variations with single pulse per cell, two stall cells ($T_{CR} = 2T_{OSC}$).

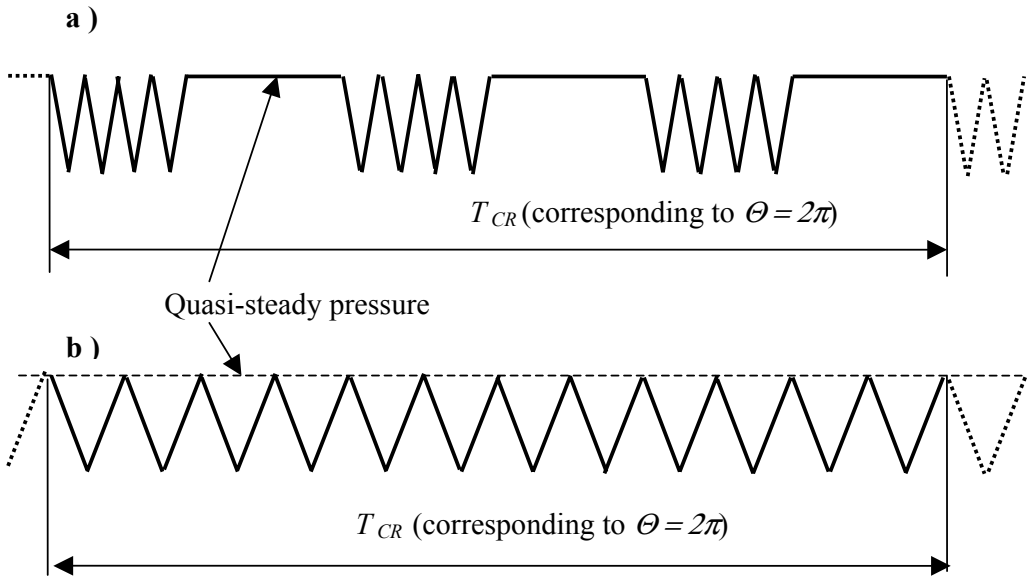


Fig. 3. Examples of distinction between different cases of pressure oscillation

a) Case of three sets of pressure decreasing which four pulses in each set.

b) Case of twelve continuously pulses in the compressor circumference.

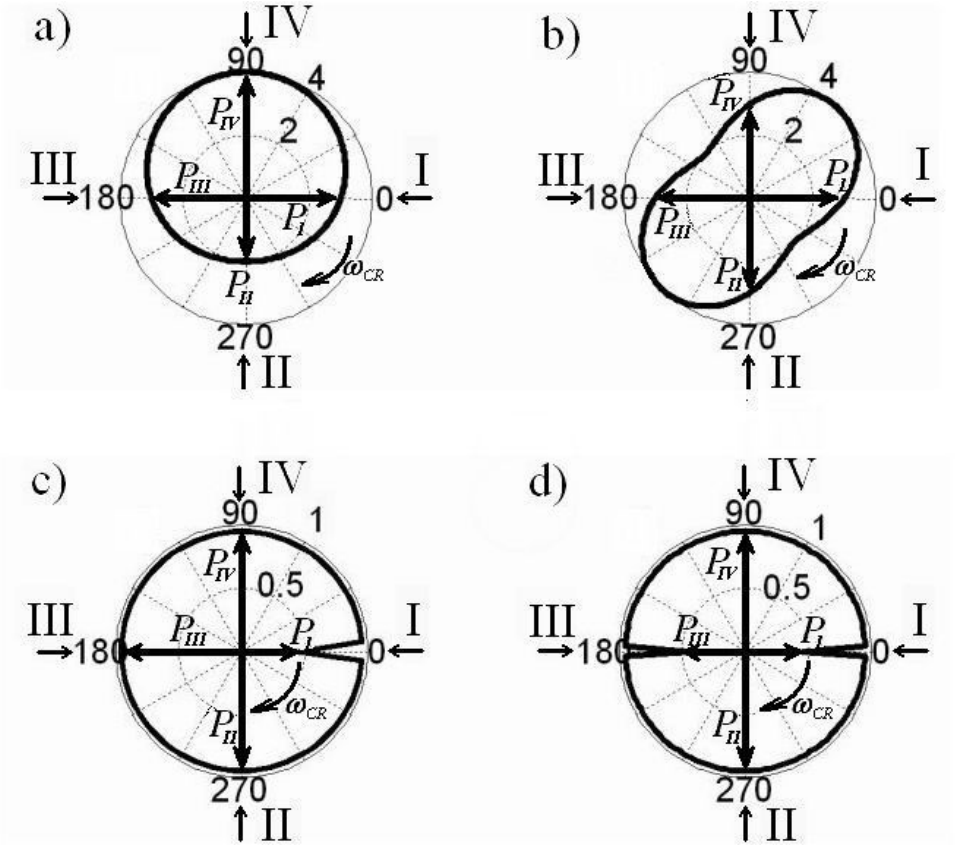


Fig. 4. Pressure fields from positions of four pressure sensors (I, II, III, IV)

a) with one stall cell of sinusoidal form ($T_{CR} = T_{OSC}$);
b) with two stall cells of sinusoidal form ($T_{CR} = 2T_{OSC}$);
c) with one stall cell of pulse form ($T_{CR} = T_{OSC}$);
d) with two stall cells of pulse form ($T_{CR} = T_{OSC}$).

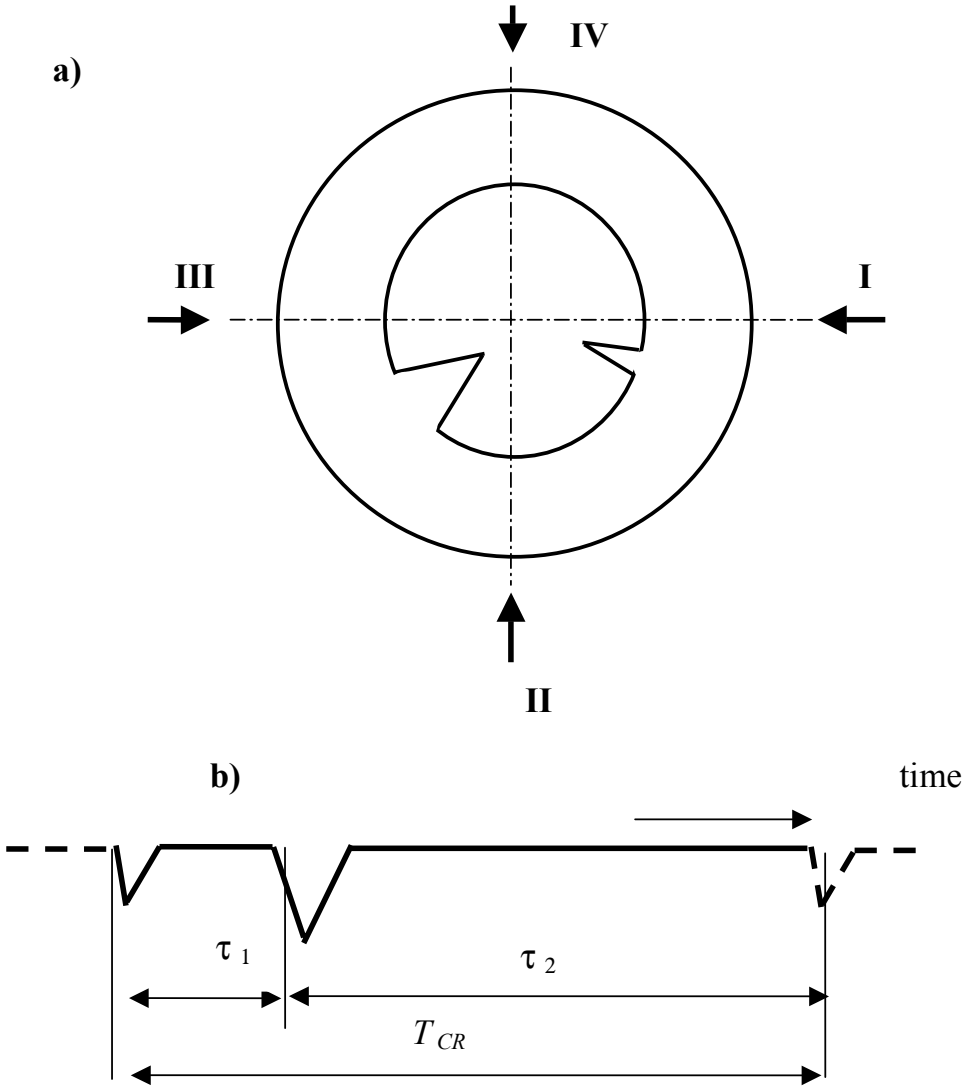


Fig. 5. The pressure values as seen by the different sensors (I, II, III, IV)
a) at the certain time and b) during time duration by one from sensors.
Example of two asymmetry stalls of pulse form.

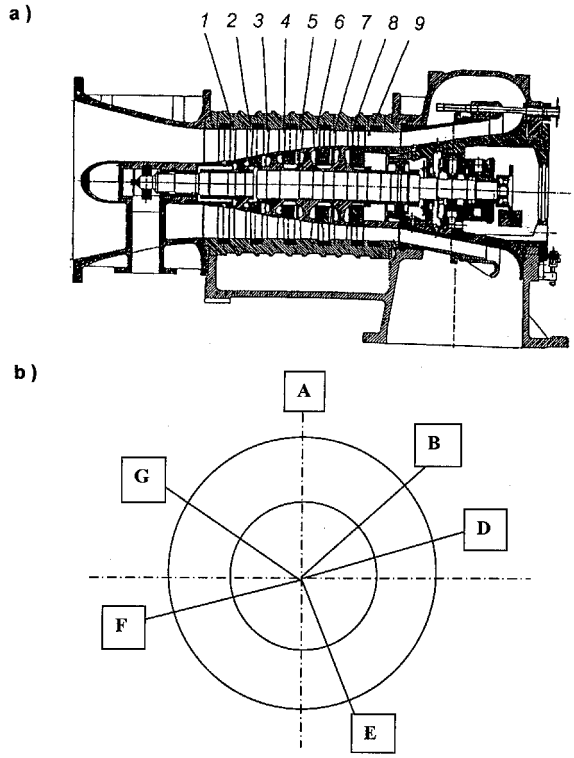


| Cross-section | A | B4 | B5 | D | E | F | G |
|---|---|---|---|---|---|---|---|
| degree | 0 | 43 | 47 | 71 | 162 | 255 | 301.5 |

Fig. 6. Diagram of four-stage compressor and numbering of its transverse (a) and longitudinal (b) cross-sections.

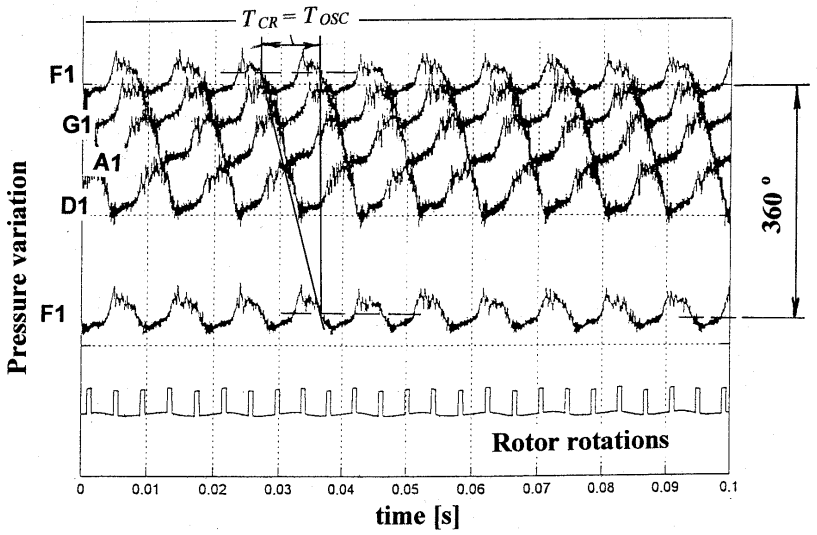


Fig. 7. Pressure variations over the circumference of compressor during an established process of rotating stall in transverse cross-section #1 (Test 8; 80% of design rotor speed).

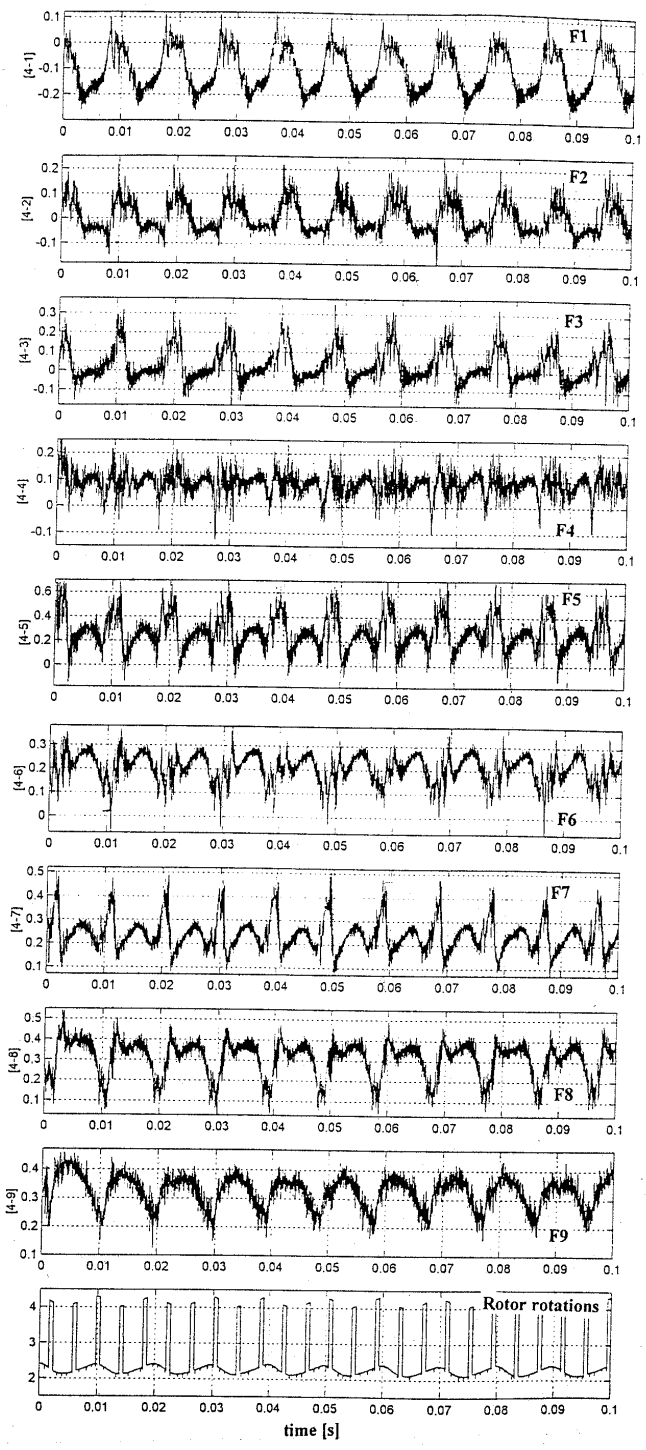


Fig. 8. Pressure periodical oscillations over the compressor length
(Test 8; 80% of design rotor speed).

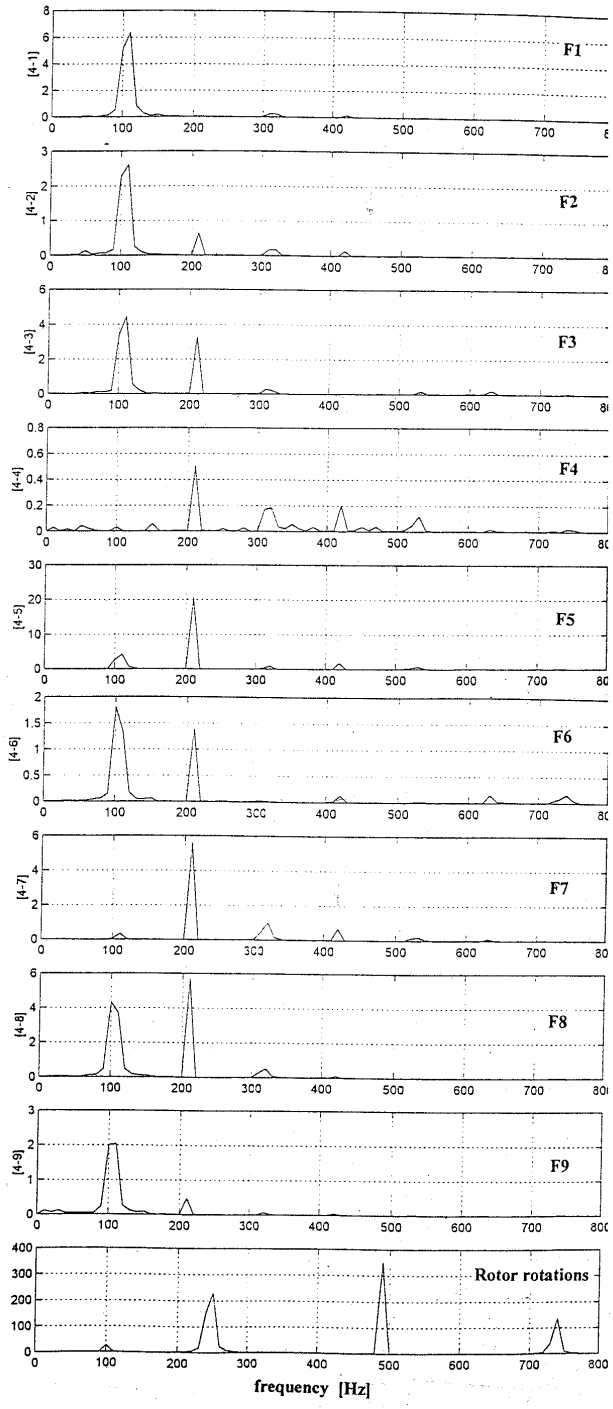


Fig. 9. Frequency spectra of the pressure signals over the compressor length (Test 8; 80% of design rotor speed).

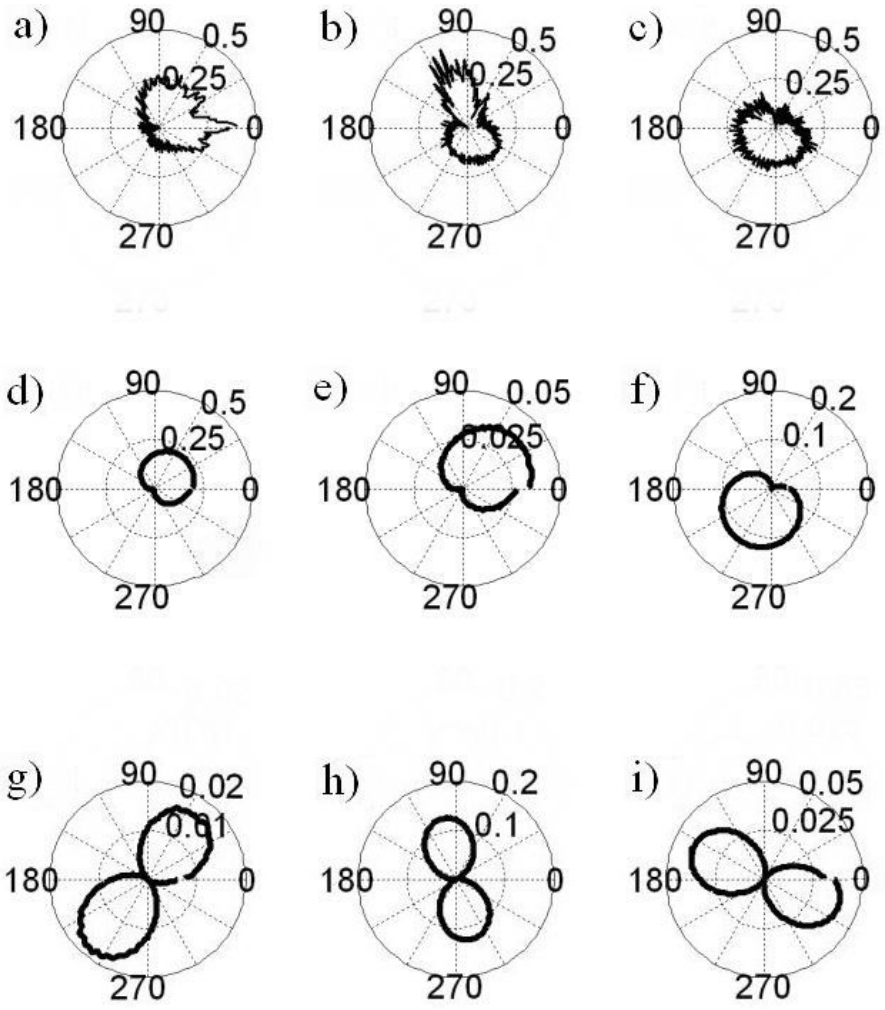


Fig.10. Visualization of the cells positions at the certain time
a, b, c - pressure signals; d, e, f - first harmonics; g, h, i - second harmonics; first vertical row (a, d, g) - in cross-section #1 *(sensor F1)*; second vertical row (b, c, h) - in cross-section #7 *(sensor F7);* third vertical row (c, f, i) - in cross-section #9 *(sensor F9)*

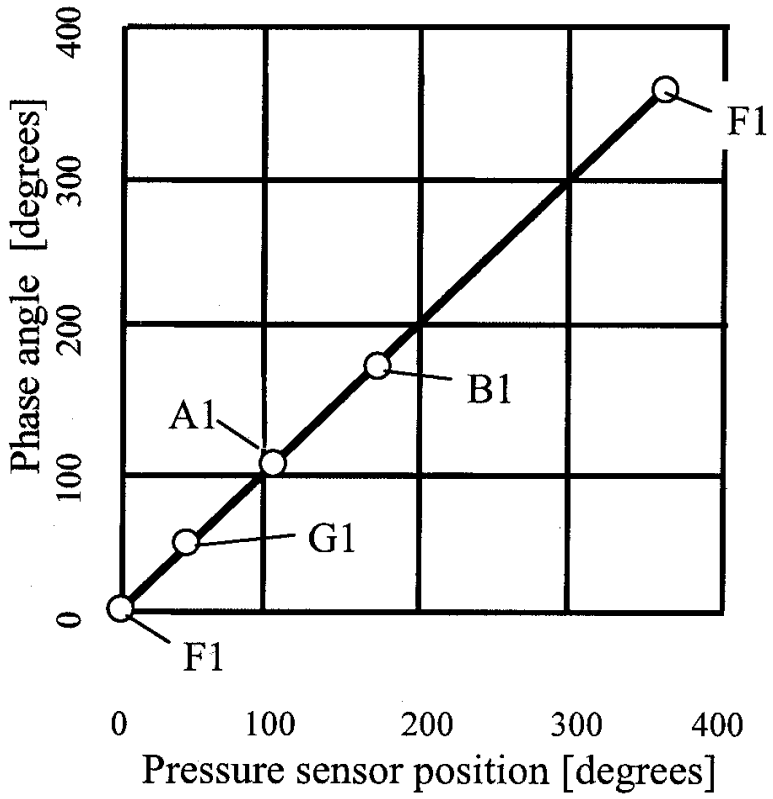


Fig. 11. Phase of first harmonic pressure signal versus positions of the sensors (G1, A1, D1 relative to sensor F1, test 9; 80% of design rotor speed).

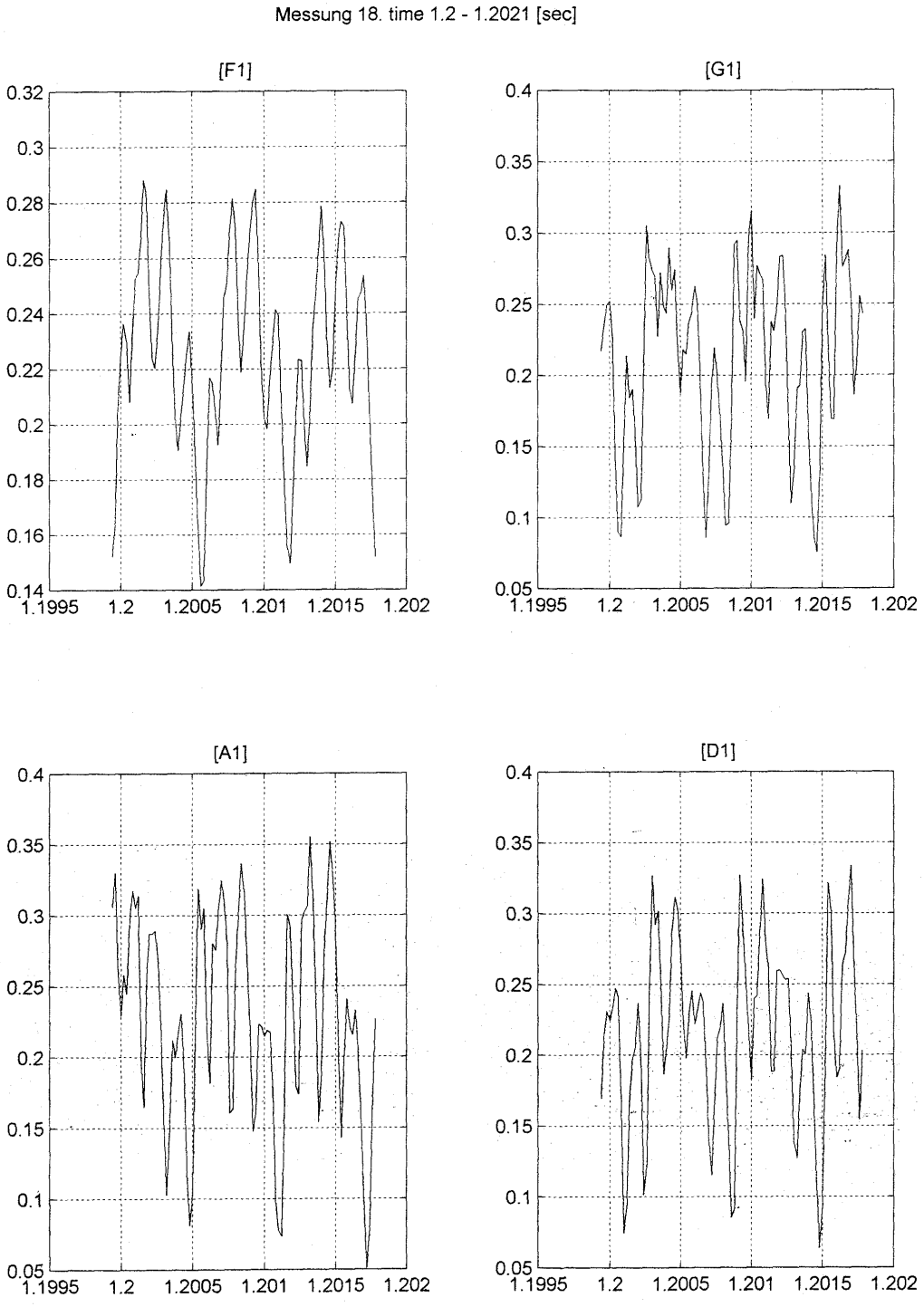


Fig. 12. Pressure variations in transverse cross-section of #1, sensors F1, G1, A1 and D1 (Test 18; 95% of design rotor speed). Horizontal axis – (time in seconds), vertical axis – pressure (in MPa)

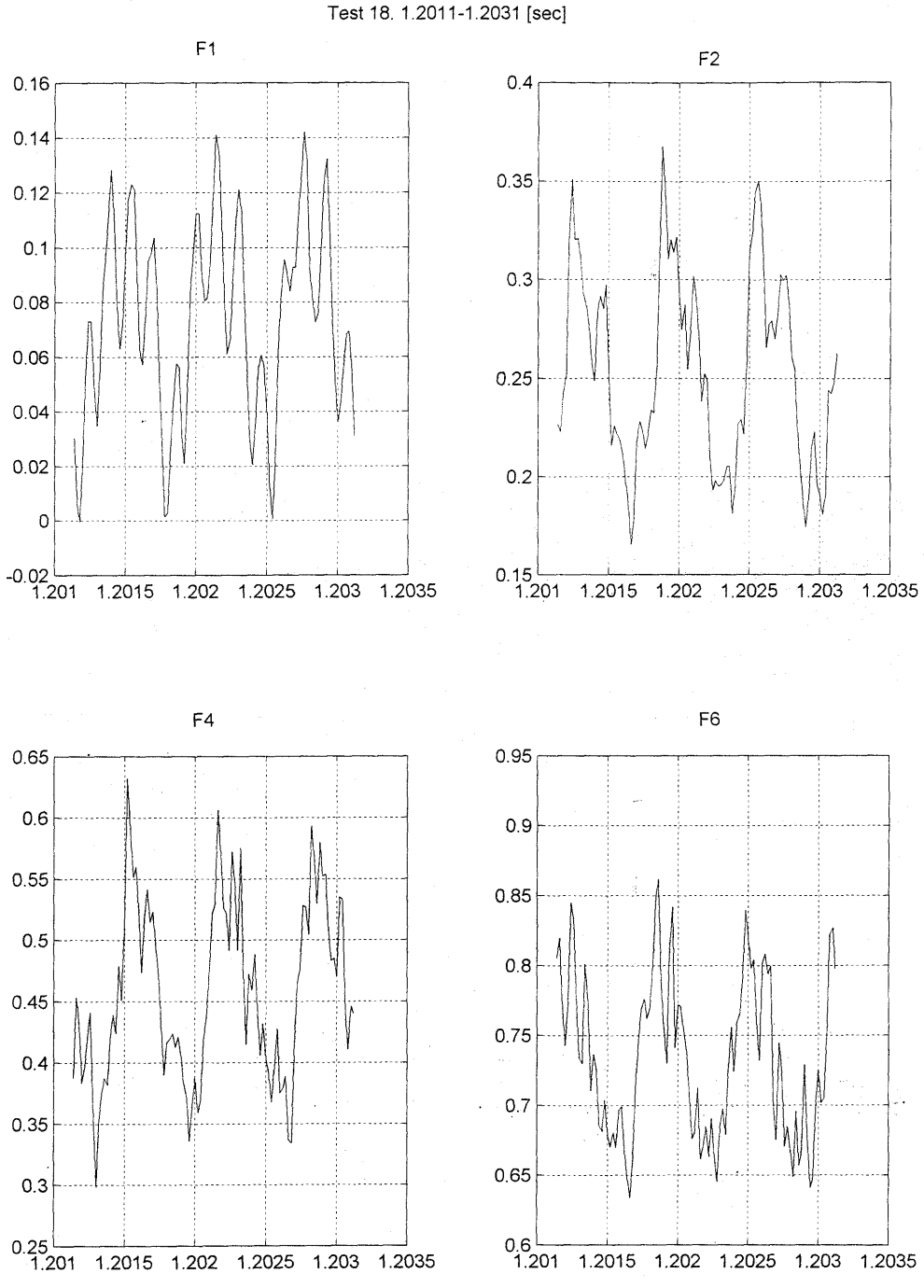


Fig. 13. Pressure variations in longitudinal cross-section *F* of the compressor, sensors F1, F2, F4 and F6. (Test 18; 95% of design rotor speed). Horizontal axis – (time in seconds), vertical axis – pressure (in MPa)

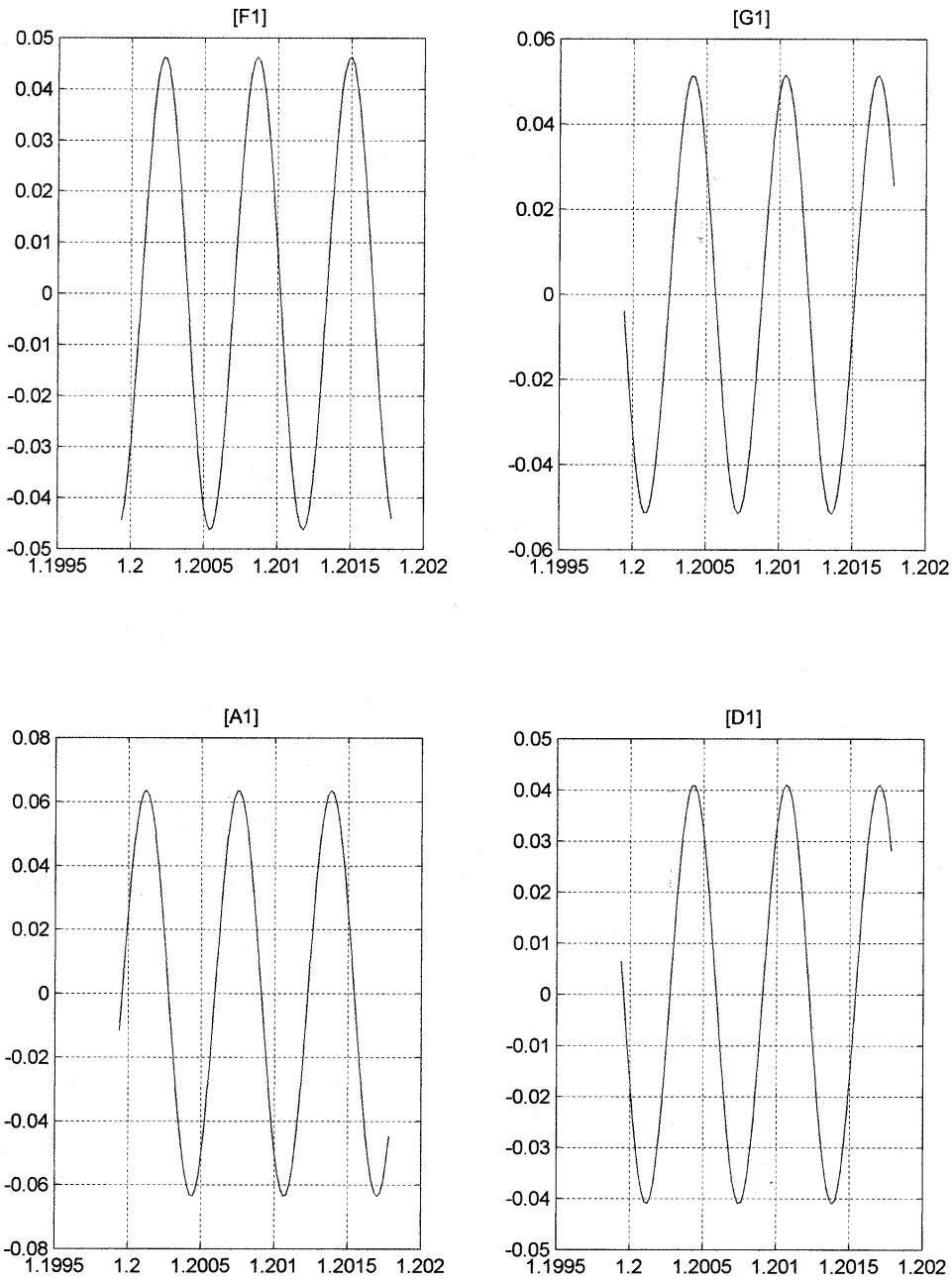


Fig. 14. First harmonics of pressure signals in transverse cross-section #1, sensors F1, G1, A1 and D1. (Test 18; 95% of design rotor speed). Horizontal axis – (time in seconds), vertical axis – pressure (in MPa

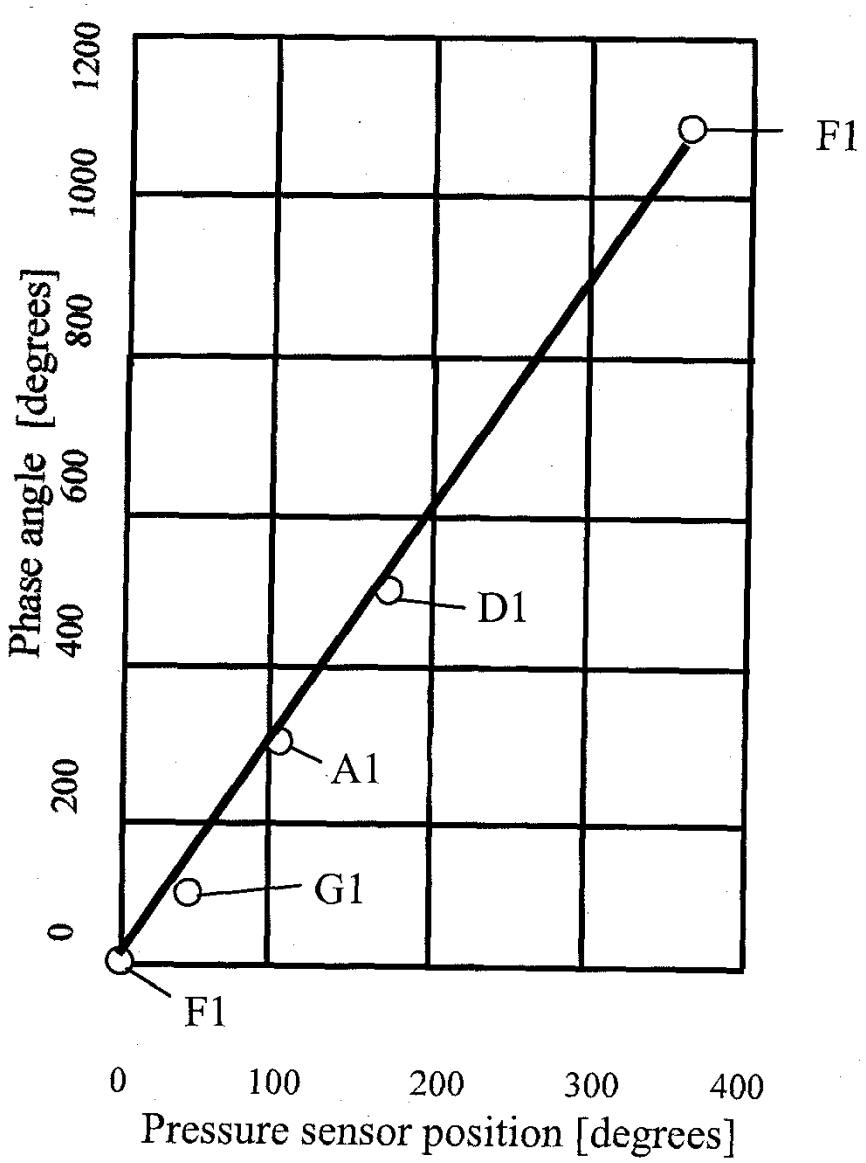


Fig. 15. Phase of first harmonic pressure signal versus positions of the sensors (G1, A1, D1 relative to sensor F1, test 18; 95% of design rotor speed).

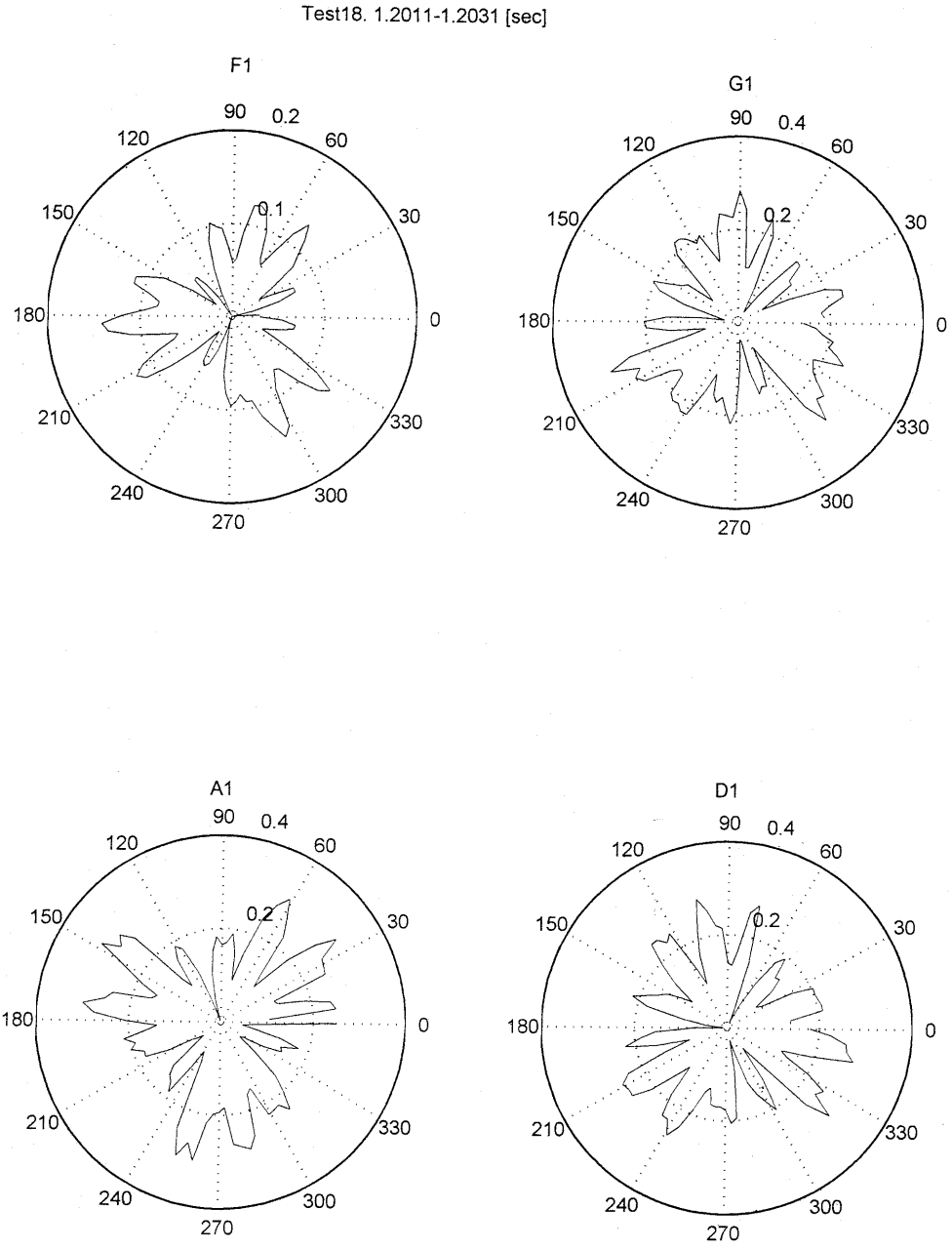


Fig. 16. Pressure variations in transverse cross-section #1 in polar coordinates (Test 18; 95% of design rotor speed).

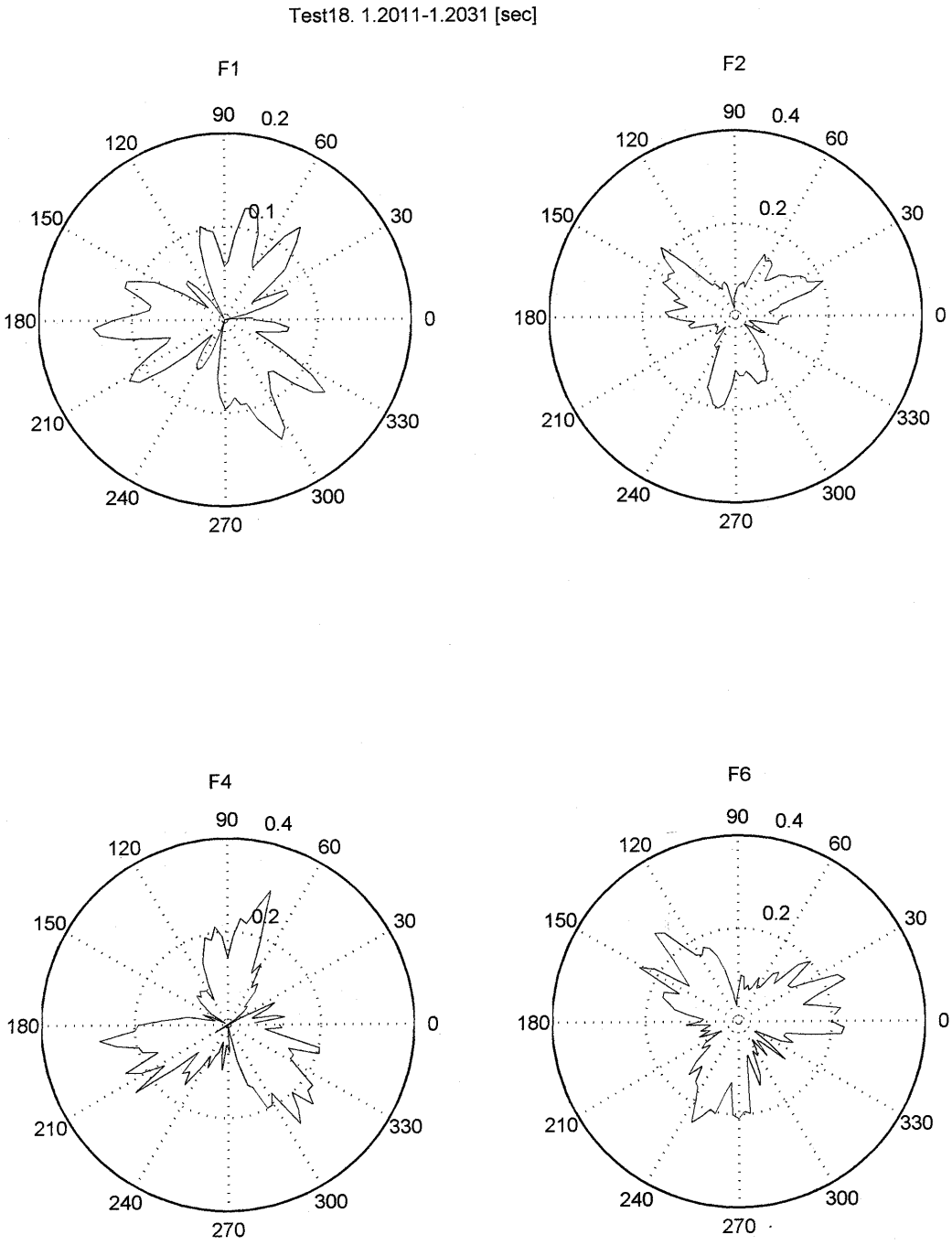


Fig. 17. Pressure variations in longitudinal cross-section in polar coordinates
(Test 18; 95% of design rotor speed).

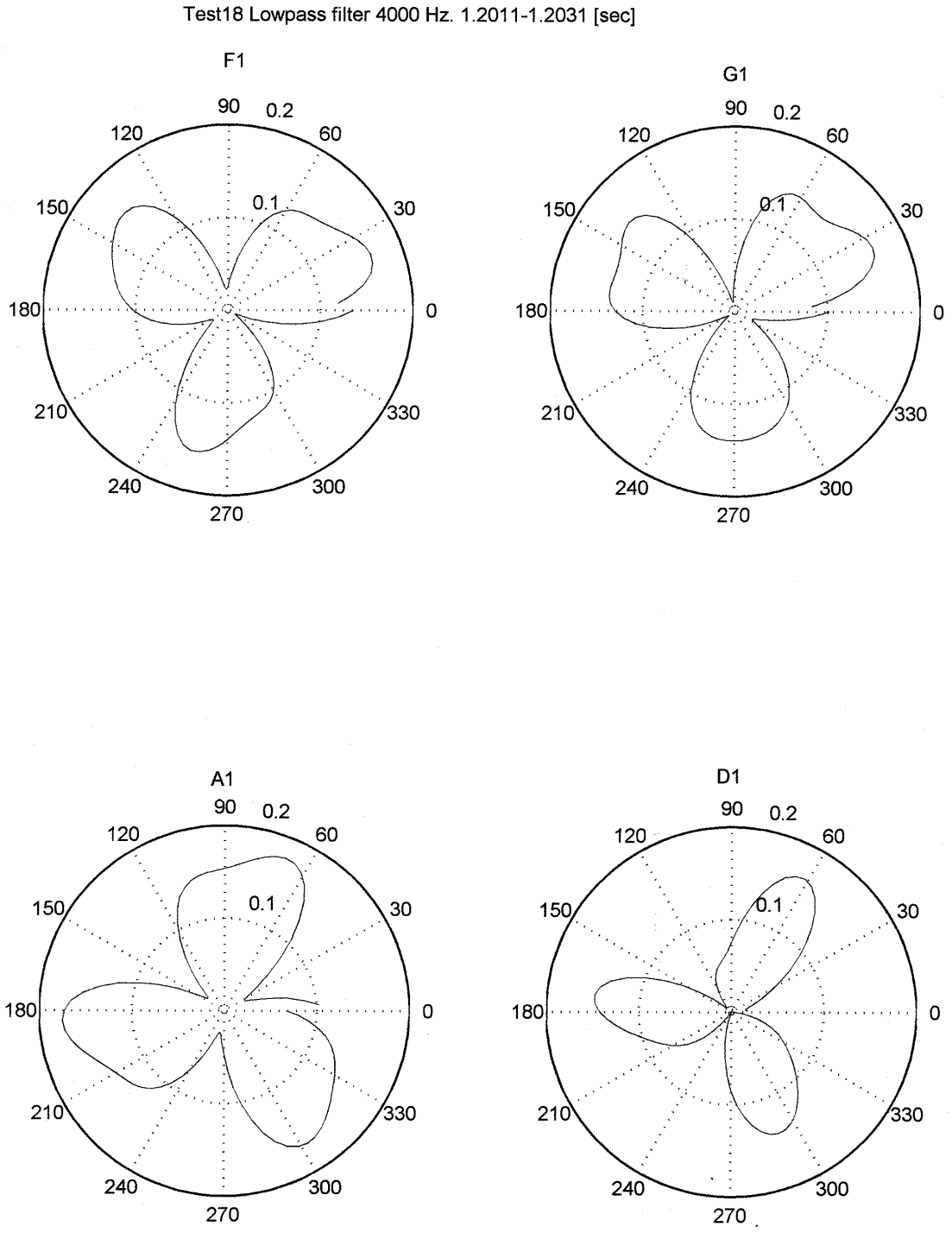


Fig. 18. First harmonics of pressure variations in transverse cross-section #1
(in polar coordinates, test 18; 95% of design rotor speed).

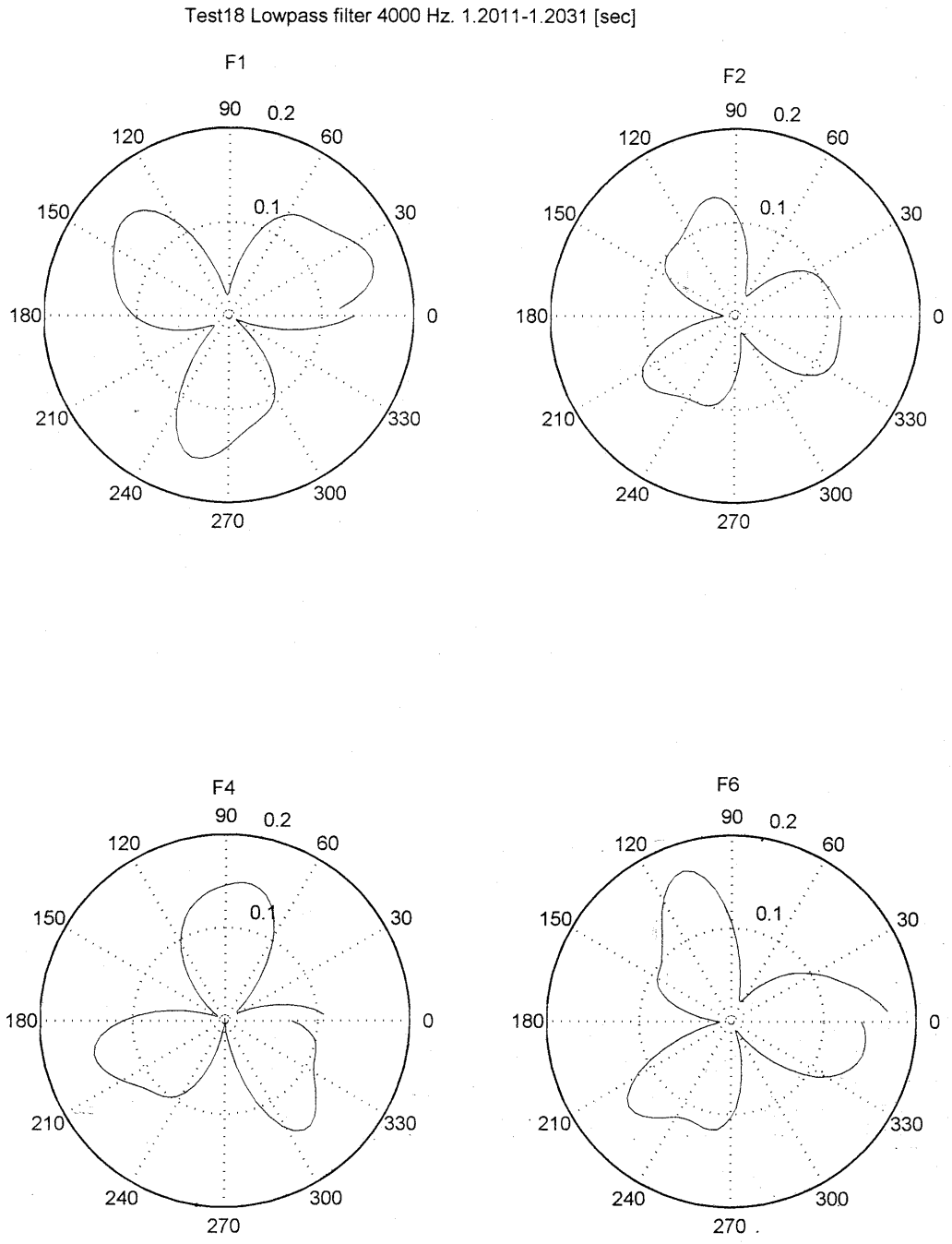


Fig. 19. First harmonics of pressure variations in longitudinal cross-section (in polar coordinates, test 18; 95% of design rotor speed).

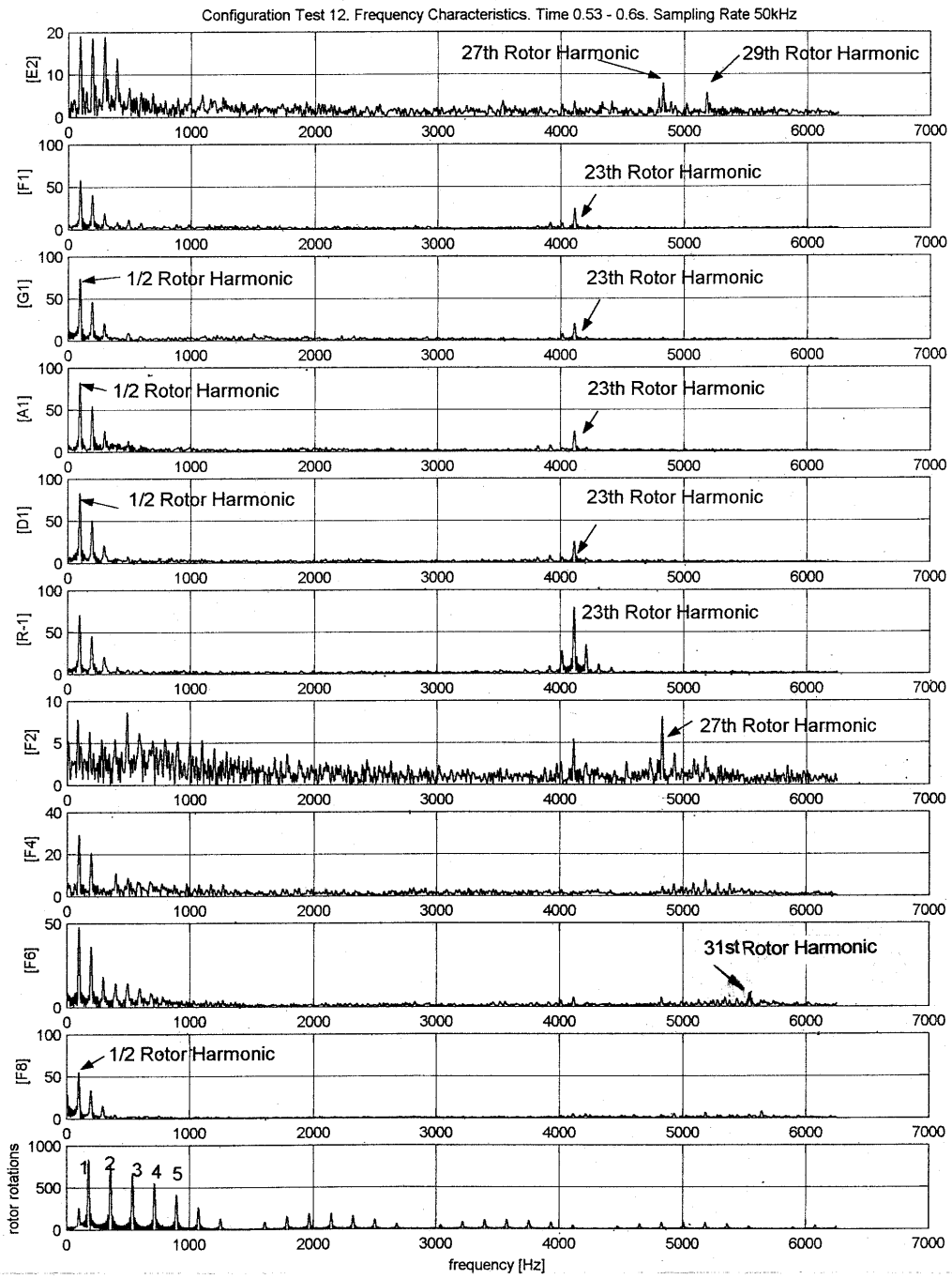


Fig. 20. Frequency spectra of the pressure signals in compressor during rotating stall (Test 12; 60% of design rotor speed).

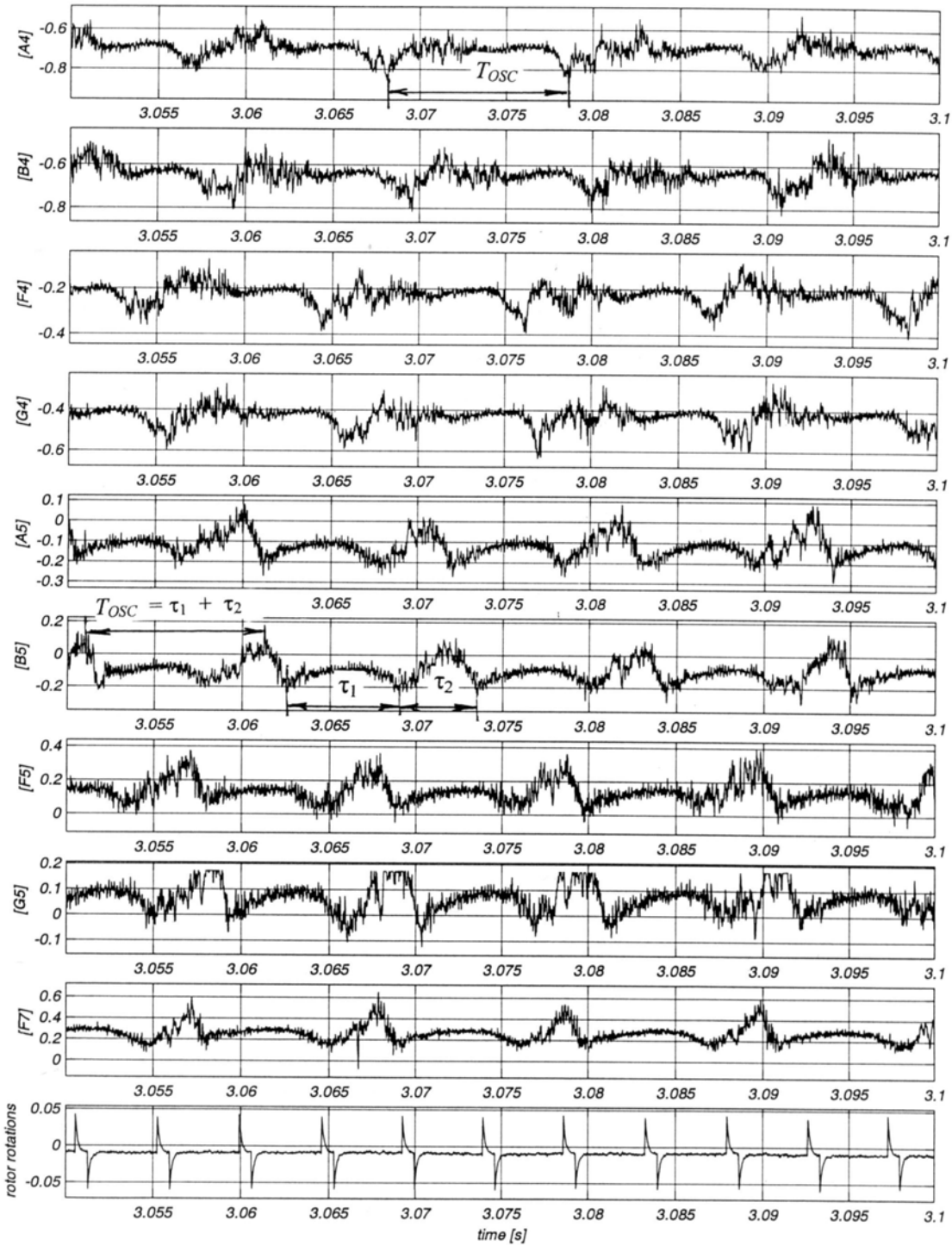


Fig. 21. Pressure variations during rotating stall
(Test K5-70-1; 70% of design rotor speed)

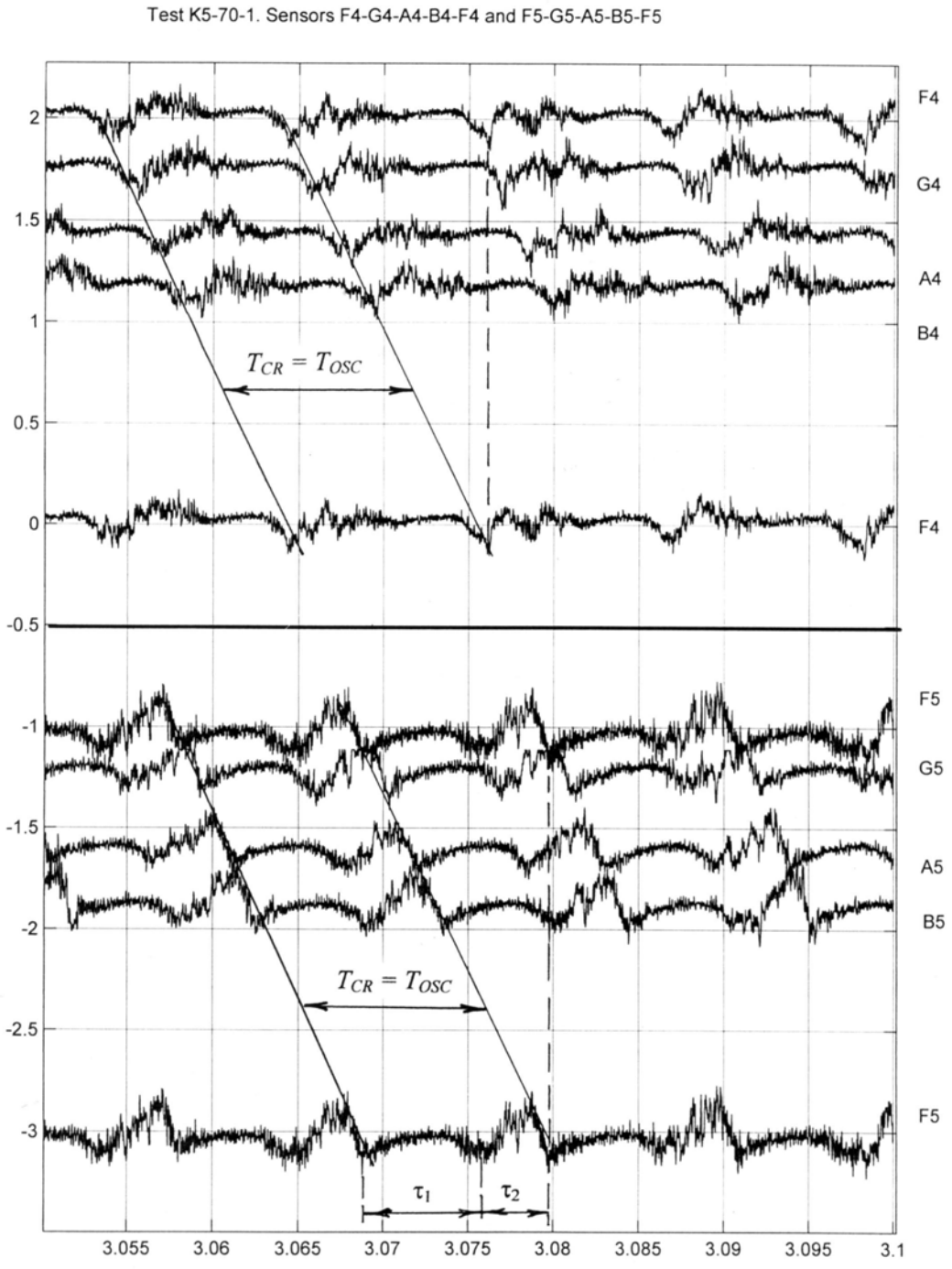


Fig. 22. Pressure variations over the compressor circumference during rotating stall in transverse cross-sections #4 (sensors F4, G4, A4, B4 with repetition of sensor F4) and #5 (sensors F5, G5, A5, B5 with repetition of sensor F5).
(Test K5-70-1; 70% of design rotor speed)

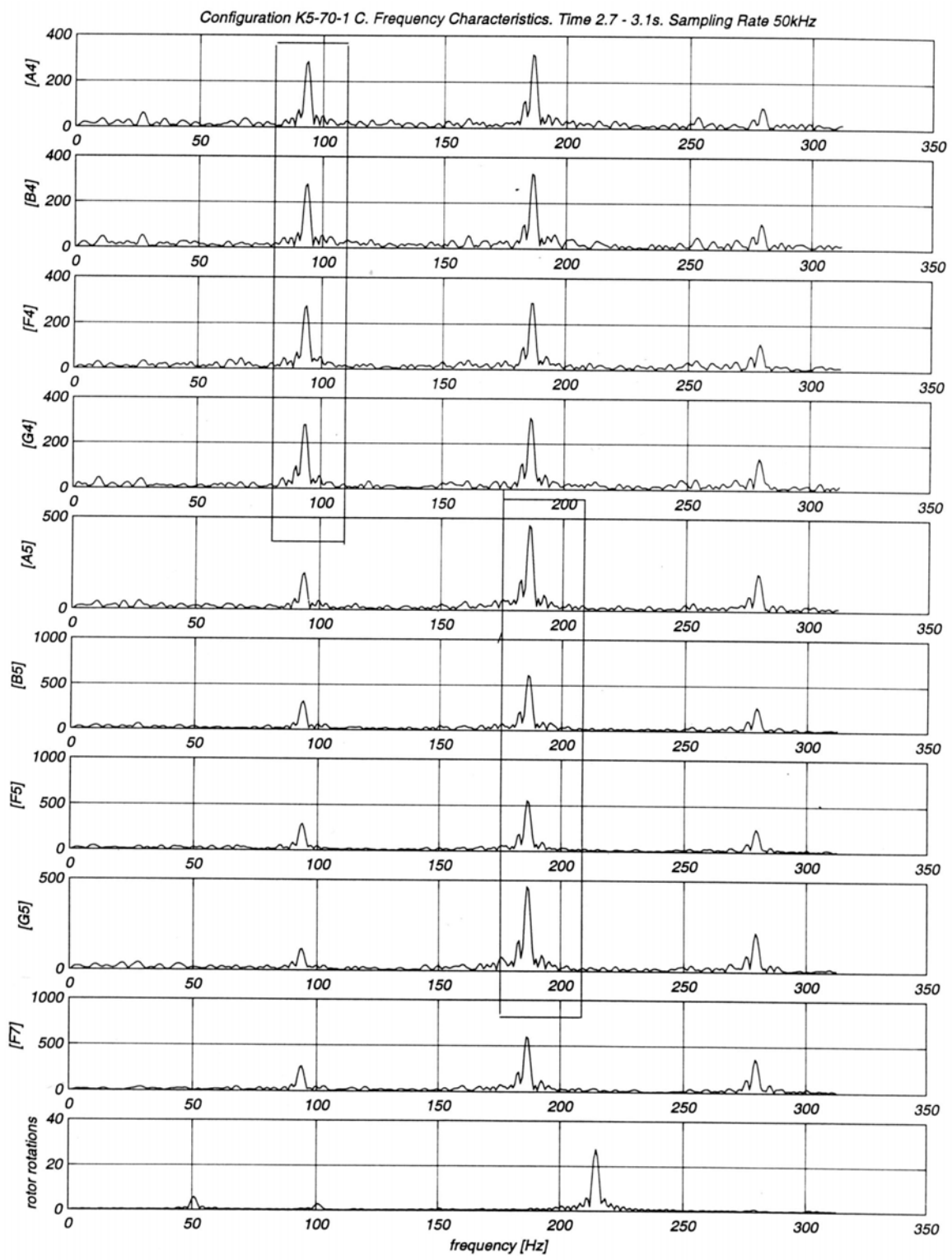


Fig. 23. Frequency spectra of the pressure signals
(Test K5-70-1; 70% of design rotor speed)

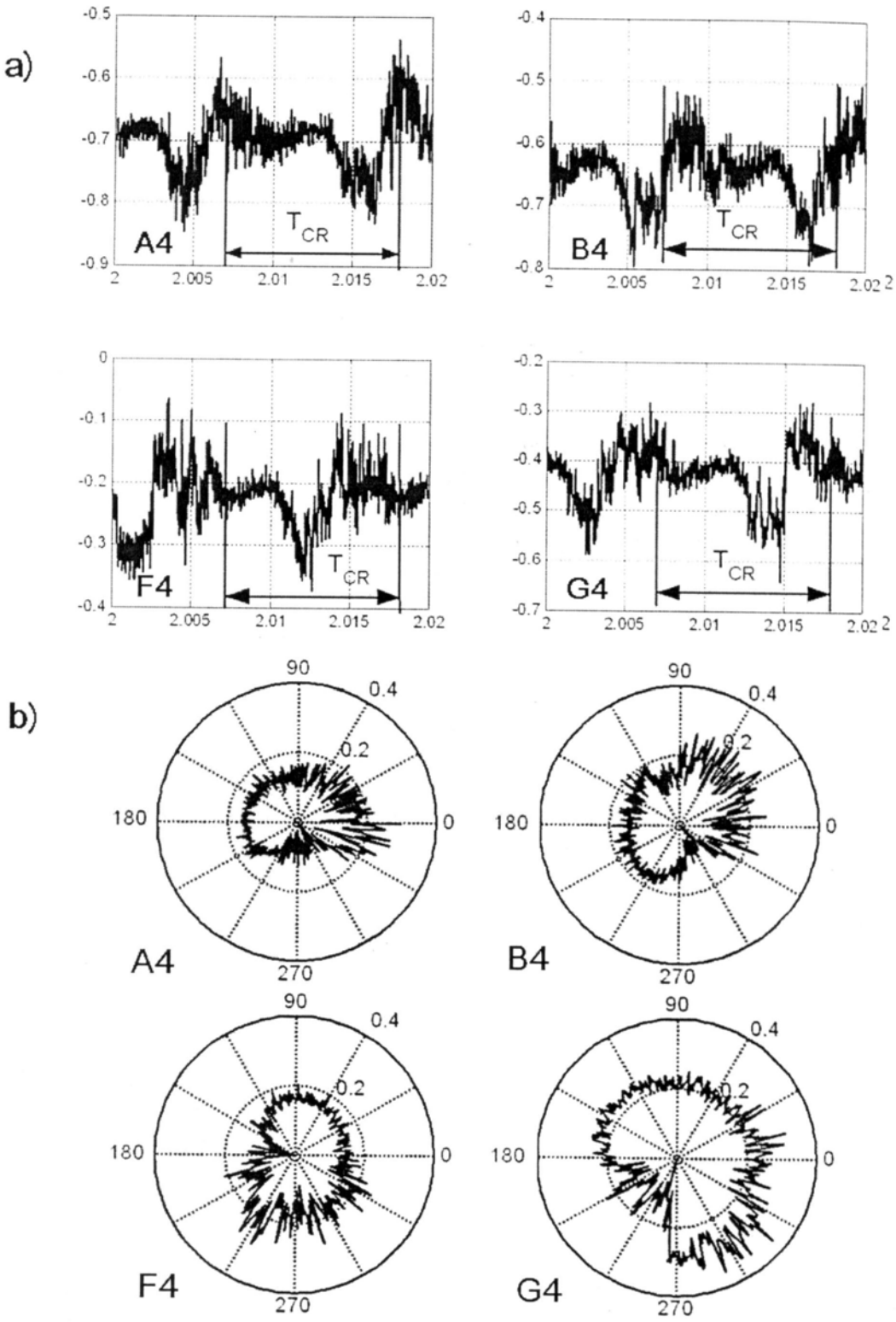


Fig. 24. Pressure signals in cross-section #4 (a – in time coordinates; b – in polar coordinates). (Test K5-70-1; 70% of design rotor speed)

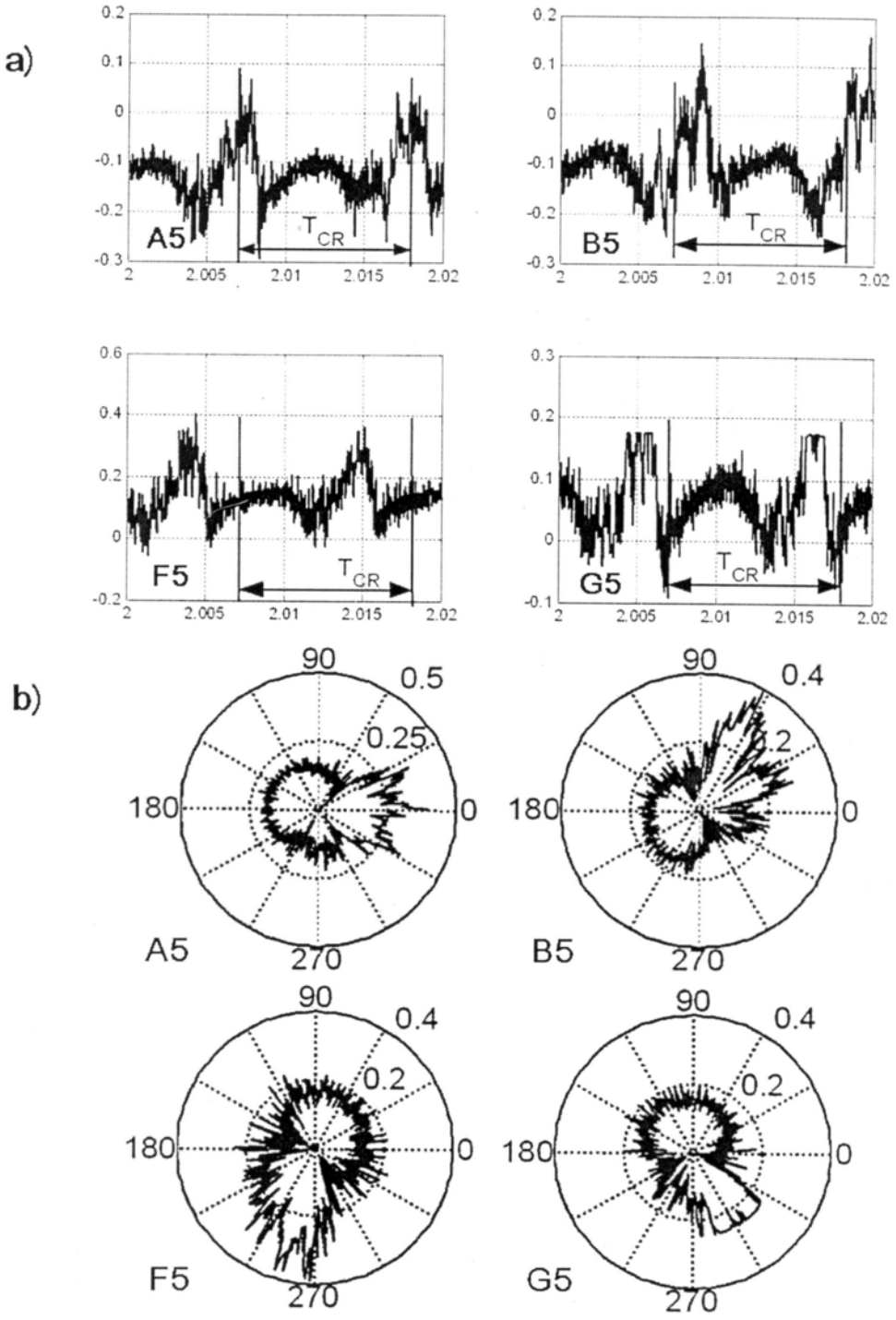


Fig. 25. Pressure signals in cross-section #5 (a – in time coordinates; b – in polar coordinates). (Test K5-70-1; 70% of design rotor speed)

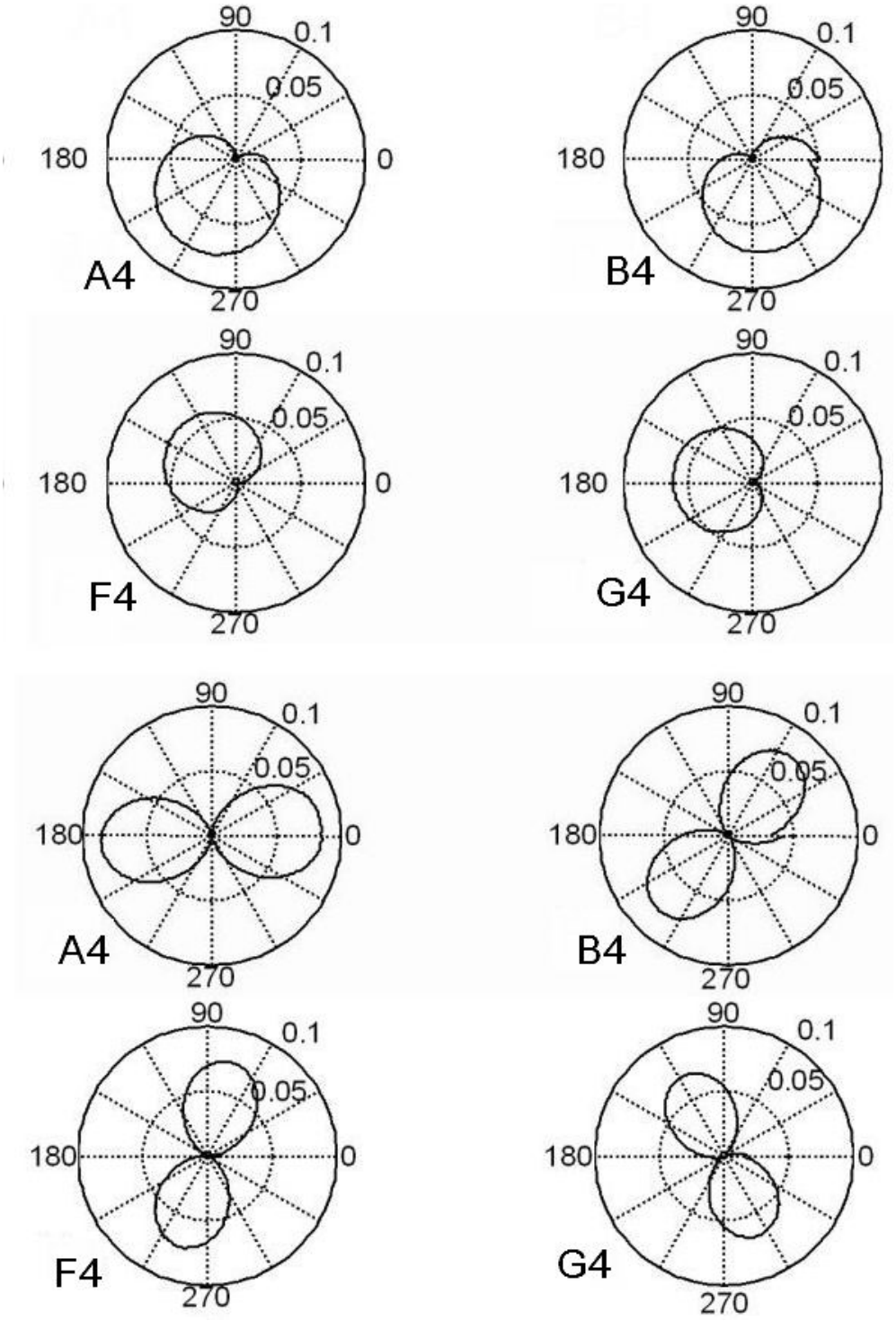


Fig. 26. Filtered pressure signals in cross-section #4 in polar coordinates (four upper diagrams – for the first harmonic; four lower diagrams – for the second harmonic) (Test K5-70-1; 70% of design rotor speed)

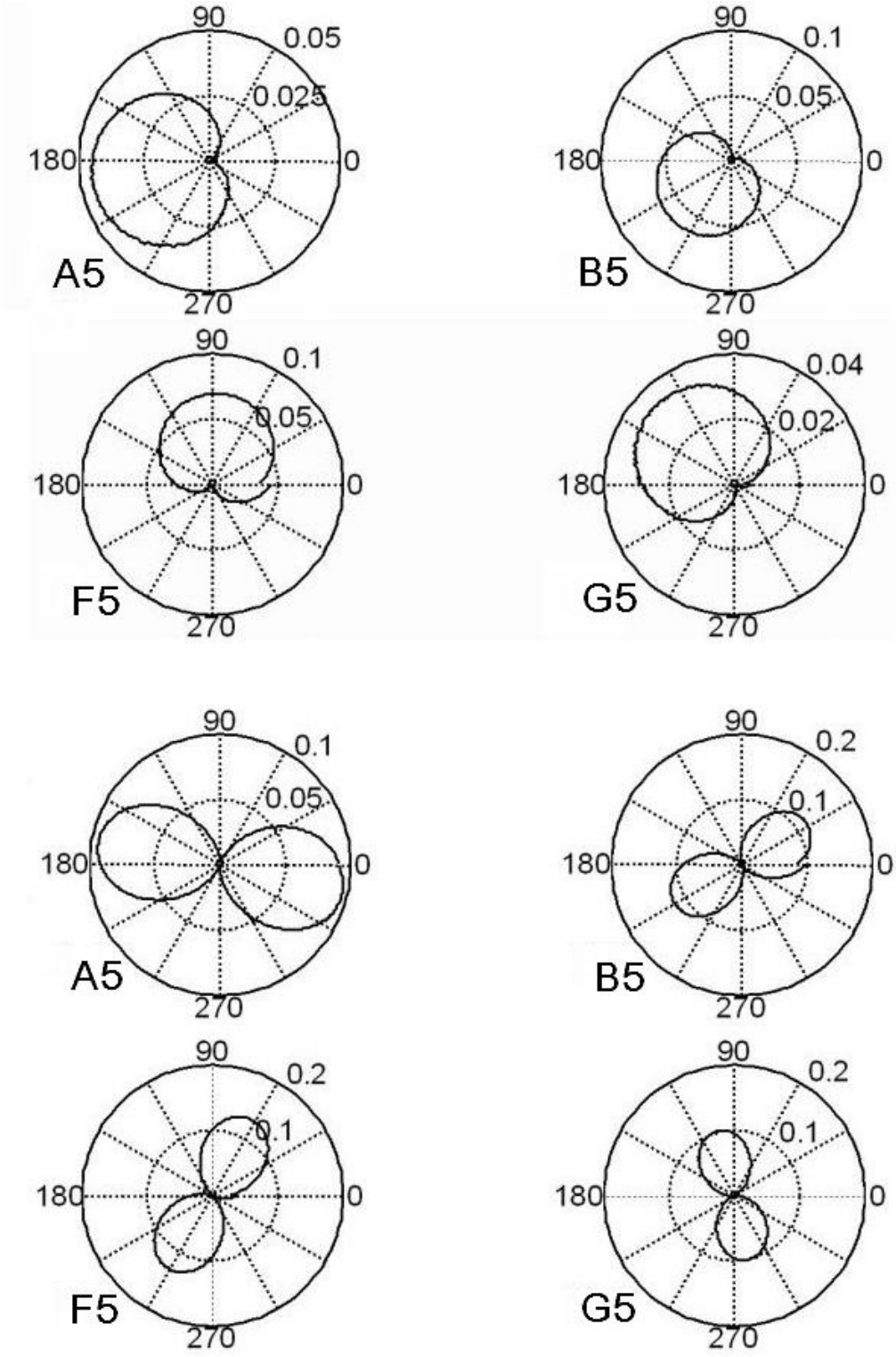


Fig. 27. Filtered pressure signals in cross-section #5 in polar coordinates (four upper diagrams – for the first harmonic; four lower diagrams – for the second harmonic) (Test K5-70-1; 70% of design rotor speed)

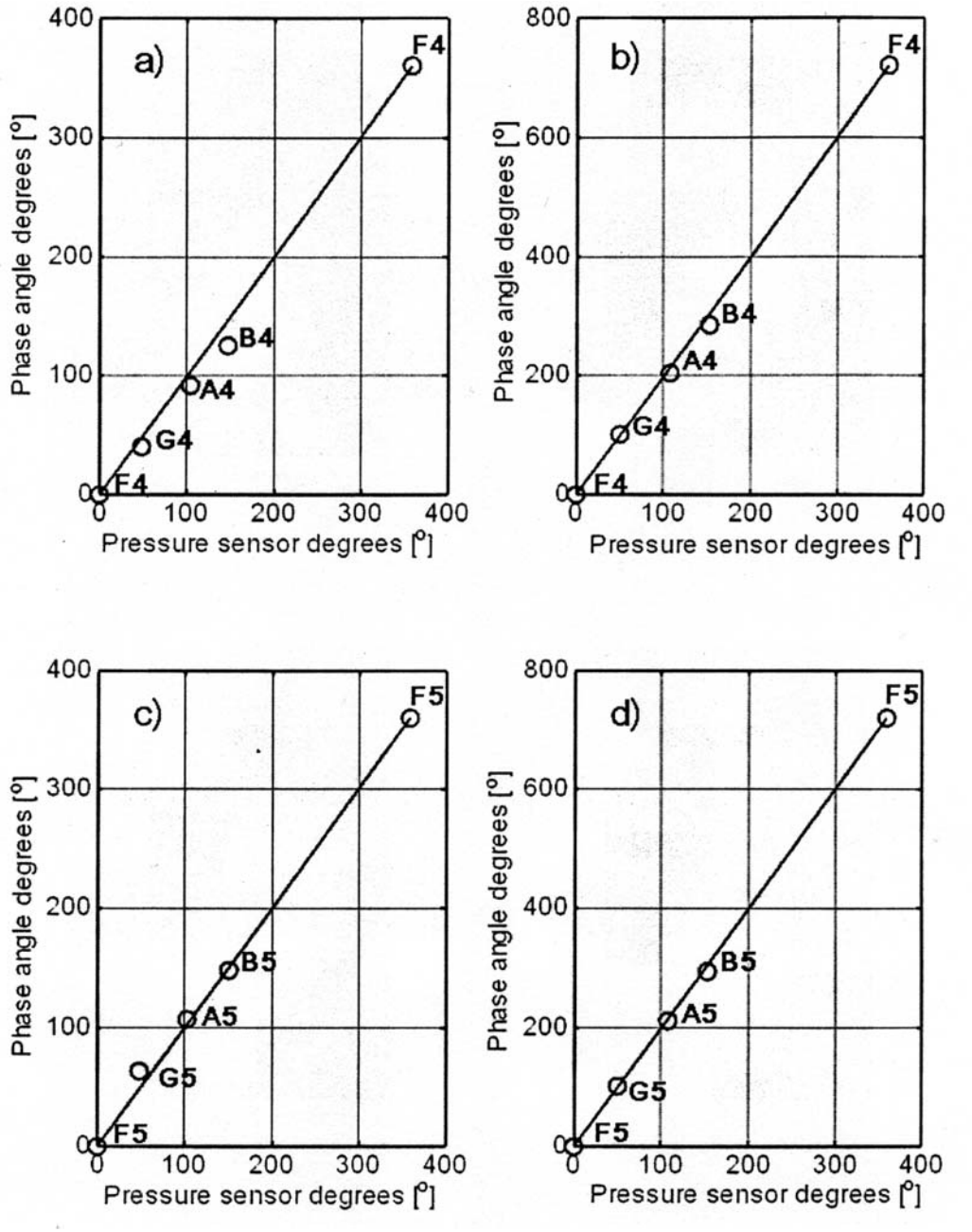


Fig. 28. Correlation between the positions of positions of sensors G4, A4, B4 relative to sensor F4 (a, b) and sensors G5, A5, B5 relative to sensor F5 (c, d) and changes of phases of pressure oscillations in these cross-sections (a, c – for first harmonic; b, d - for second harmonic). (Test K5-70-1; 70% of design rotor speed)